Quaternary Science Reviews 317 (2023) 108257

Contents lists available at ScienceDirect

Quaternary Science Reviews

journal homepage: www.elsevier.com/locate/quascirev

By the lakeshore: Multi-scalar geoarchaeology in the Turkana Basin at GaJj17, Koobi Fora (Kenya)

Kathryn L. Ranhorn [a,b,*], Silindokuhle S. Mavuso [c,d], Debra Colarossi [e,g], Tamara Dogandžić [f,g], Kaedan O'Brien [h,i], Mathilde Ribordy [j], Christopher Ssebuyungo [k,l], Shannon Warren [m], John W.K. Harris [n], David R. Braun [o,p], Emmanuel Ndiema [n]

[a] Institute of Human Origins, Arizona State University, Tempe, AZ, USA
[b] School of Human Evolution and Social Change, Arizona State University, Tempe, AZ, USA
[c] Department of Geology, Rhodes University, Makhanda (Grahamstown), South Africa
[d] School of Geosciences, University of the Witwatersrand, Johannesburg, South Africa
[e] Department of Geography and Earth Sciences, Aberystwyth University, Aberystwyth, Wales, UK
[f] MONREPOS Archaeological Research Centre and Museum for Human Behavioral Evolution, Schloss Monrepos, Neuwied, LEIZA, Germany
[g] Department of Human Evolution, Max Planck Institute for Evolutionary Anthropology, Deutscher Platz 6, 04103, Leipzig, Germany
[h] Department of Anthropology, University of Utah, Salt Lake City, USA
[i] Natural History Museum of Utah, Salt Lake City, USA
[j] Department of Anthropology, Department of Human Evolutionary Biology, Harvard University, Cambridge, MA, USA
[k] Uganda National Museum, Kampala, Uganda
[l] Department of History, Archaeology and Heritage Studies, Makerere University, Kampala, Uganda
[m] Department of Geology, University of Kansas, Lawrence, USA
[n] Department of Earth Sciences, National Museums of Kenya, Nairobi, Kenya
[o] Technological Primate Research Group, Max Planck Institute for Evolutionary Anthropology, Deutscher Platz 6, 04103, Leipzig, Germany
[p] Center for the Advanced Study of Human Paleobiology, Department of Anthropology, George Washington University, Washington, DC, USA

ARTICLE INFO

Handling editor: Claudio Latorre

Keywords:
Africa
Archaeology
Optically stimulated luminescence
Paleoenvironment
Quaternary
Site formation

ABSTRACT

The Late Pleistocene archaeological record in the Turkana Basin is important for studying *Homo sapiens* evolution, but the record in this region is poorly documented, despite a long history of significant paleoanthropological discoveries. Ambiguity around ages and site formation processes are paramount problems. We investigated the chronometric, geological, archaeological, and paleoenvironmental context of GaJj17, a locality with an artifact-bearing deposit in the Koobi Fora region. Sedimentological facies analysis coupled with micromorphological evidence indicate the depositional environment at the site changed over time from a fluvial system to an aeolian one, forming the remnant lunate feature seen today. Caliche caps the site and likely mitigated erosion of the site during high lake stands; similar deposits (~25 m^2) are found within a 2 km radius and are archaeologically sterile. Optically stimulated luminescence dating indicates the deposit and associated artifacts and fossils were emplaced circa 52–43 thousand years ago. Small (average length ~ 3.5 cm) flakes dominate the stone artifact assemblage and include unretouched triangular flakes on diverse raw materials indicating shared affinity with Middle and Late Pleistocene lithic toolkits elsewhere in eastern Africa. Hippopotamus, crocodiles, and fish are well-represented in the faunal assemblage, along with a small sample of terrestrial ungulate specimens. More taphonomic research to understand the accumulating agent(s) of the faunal assemblages is needed. These results contribute to our understanding of Late Pleistocene archaeological site formation processes in lacustrine contexts of the Omo-Turkana Basin.

1. Introduction

The tectonically active lake basins of the East African Rift System (EARS) formed important linkages and barriers along which Pleistocene human populations may have lived, migrated, and/or interacted. Lake levels fluctuated significantly, over 70 m in the Turkana basin during the

* Corresponding author. PO Box 872402 Tempe, AZ, 85287 USA.
E-mail address: kathryn.ranhorn@asu.edu (K.L. Ranhorn).

https://doi.org/10.1016/j.quascirev.2023.108257
Received 11 April 2023; Received in revised form 20 July 2023; Accepted 3 August 2023
Available online 28 August 2023

Holocene alone (Bloszies et al., 2015). Understanding how local floral and faunal communities shifted in response, and how Pleistocene humans adapted to these dynamic lake environments, is important to building human adaptive capacity to climate change (SDG 13). Much of current understanding regarding Late Pleistocene *Homo sapiens* behavior, however, derives from caves and rock shelter deposits comprising relatively long stratigraphic sequences at a single locality, for example, at Kisese II (Patania et al., 2022; Ranhorn et al., 2023), Enkapune Ya Muto (Ambrose, 2002; Leplongeon, 2016; Marean, 1992; Marean et al., 1994), Mumba Rockshelter (Bushozi et al., 2020; Mehlman, 1979; Prendergast et al., 2007), Nasera Rockshelter (Mehlman, 1977; Ranhorn and Tryon, 2018; Solano-Megías et al., 2021), and Panga ya Saidi (d'Errico et al., 2020; Prendergast et al., 2023; Shipton et al., 2018.).

Open-air Pleistocene sites associated with *Homo sapiens* in EARS contexts are less common; variation in and ambiguity around depositional history and geochronology have largely precluded landscape scale time-transgressive comparative analyses. In the Baringo Basin for example landscape scale research in the Kapthurin Formation showed human technological innovation in stone tool technology spanning 400+ kyr (McBrearty and Tryon, 2006; Tryon, 2010; Tryon and McBrearty, 2002; Tryon et al., 2006). Research near the Omo River depicted fossil evidence of *Homo sapiens* dated around 222 ka (Vidal et al., 2022) and diverse manufacture of lithic technology (Shea, 2008). Several localities in the Lake Victoria Basin (Blegen et al., 2015; Tryon et al., 2014) underscore the significance of lacustrine environments for Late Pleistocene human populations, and work in the Nile River Valley (Davis, 2019; Garcea, 2022; Vermeersch and Van Neer, 2015) demonstrate a deep history of human reliance on riverine resources. All these examples demonstrate the importance of detailed site-level observations for building broader landscape-scale understandings of human-environment interaction throughout the dynamic climate changes of the later Pleistocene.

In the Turkana Basin over forty years of geological and paleontological research has documented a record spanning ca. 4 million years of human evolution and behavioral change (Bobe and Behrensmeyer, 2004; Isaac et al., 1971; Leakey, 1970; Leakey et al., 1978). Despite its extensive geological record, the Middle and Late Pleistocene (781–126 and 126–11.7 ka respectively; Cohen et al., 2013) is not well documented in Turkana due both to preservation bias and relatively limited research (Kelly, 1996a, 1996b; Kelly and Harris, 1992; Shea and Hildebrand, 2010). GaJj17 (3.96° N, 36.30° E) is a unique locality located in the Koobi Fora region near Lake Turkana (Fig. 1) where faunal and archaeological evidence in primary context records hominin behavior in a lakeshore environment. In this paper, we combine multiple lines of evidence to build a multi-scalar reconstruction of site formation processes through time, with a specific focus on depositional environment and taphonomy. The geological, archaeological, faunal, and dating evidence derived from our excavations at GaJj17 demonstrate a) hominin presence in a lakeshore environment ca. 52–43 ka and b) the need for multi-scalar taphonomy-oriented geoarchaeological studies to inform behavioral inferences.

1.1. Pleistocene geology of East Turkana

The sedimentary sequence of the East Turkana region provides a unique opportunity to investigate geological and ecological change over the last four million years. The paleontological and archaeological remains associated with these deposits are marked by transitions attributed to global and regional climate, tectonics, and lake level fluctuations (Cerling et al., 2011; Feibel, 2011). These sediments, referred to as the Koobi Fora Formation of the Omo Group, have distinct stratigraphic markers with corresponding dateable volcanic tuff horizons forming a largely continuous litho-stratigraphic sequence with a high-resolution chronostratigraphic framework (Brown and Feibel, 1986; Feibel, 2011; Gathogo and Brown, 2006). The Koobi Fora Formation's Plio-Pleistocene record provides crucial contextual evidence for investigations into the taxonomic diversity and ecological disparity of

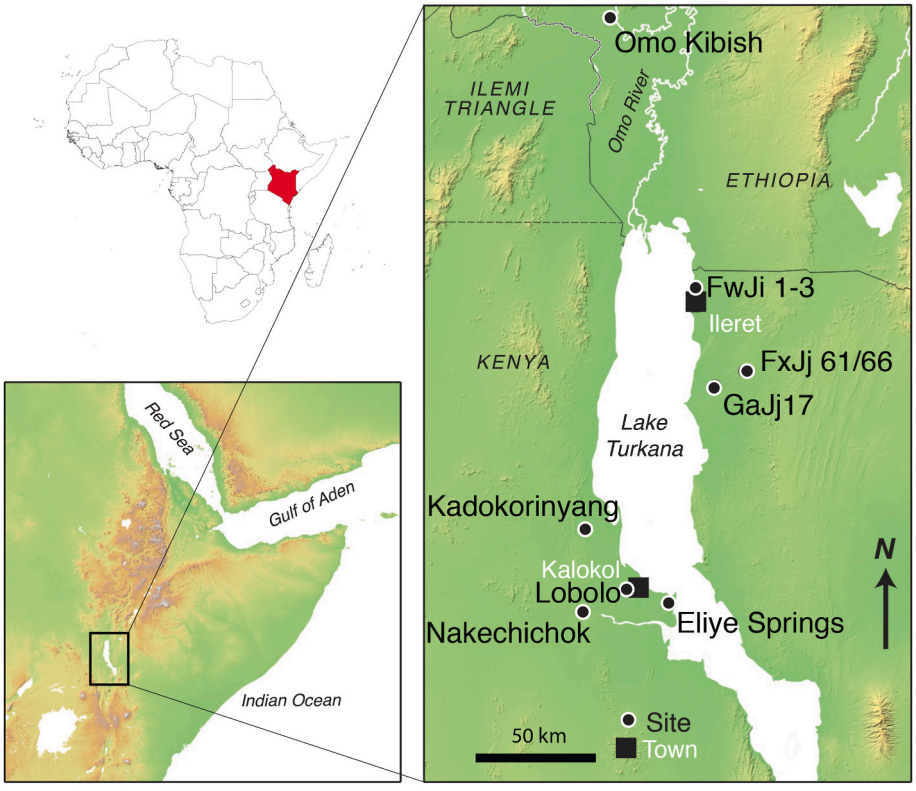

Fig. 1. Late Pleistocene archaeological sites in the Omo Turkana Basin. Digital elevation data provided by the Shuttle Radar Topography Mission (NASA). Inset) 30 arc-second digital elevation model of the East African Rift Valley (EARV) system, data from United States Geological Survey GTOPO30.

several hominin lineages, including *Paranthropus*, *Australopithecus*, and early *Homo* (cf. Wood and Leakey, 2011). The lack of documented vertically and laterally extensive Middle and Late Pleistocene deposits, however, limits the scientific investigation of the latter periods of the human evolutionary record in Turkana, including the emergence and evolution of *H. sapiens* in the region.

1.1.1. Guomde Formation geology and associated fossil hominins

Vondra et al. (1971) provided the earliest description of Middle to Late Pleistocene sediments at East Turkana, which they initially described as the "middle unit" at Ileret, disconformably overlaying what was later termed the Chari Tuff, now dated to 1.39 Ma (McDougall, 1985; McDougall and Brown, 2006). Bowen and Vondra later formally proposed the "Guomde Formation" (Bowen and Vondra, 1973:392), a stratigraphic unit overlying the Koobi Fora Formation with angular unconformity comprising tuffaceous siltstones and representing predominantly nearshore lacustrine and deltaic plain environments.

In 1971 an expedition led by the National Museums of Kenya (NMK) reported the discovery of a hominin femur, KNM-ER 999, and cranium, KNM-ER 3884, from deposits then considered part of the Guomde Formation (Brauer et al., 1992; Day and Leakey, 1974; Leakey et al., 1978; Trinkaus, 1993). Later, in 1986, Brown and Feibel argued to subsume the Guomde Formation into the Koobi Fora Formation stating that the former lacked laterally continuous deposits, a characteristic required to receive formational rank (Brown and Feibel, 1986).

While the relative context of Guomde fossils KNM-ER 999 and KNM-ER 3884 remain unconfirmed, morphological analyses suggest that both specimens are more closely related to *Homo sapiens* than to earlier members of the genus *Homo* (Brauer et al., 1992; Trinkaus, 1993). Direct U-series dating of KNM-ER 3884 suggest the specimen may date between 270 and 300 ka (Brauer et al., 1992). Recent re-dating evidence from Jebel Irhoud, Morocco suggests an age of 315 ± 34 ka for fossils that some attribute to *H. sapiens* (Hublin et al., 2017). Additionally, *H. sapiens* remains were discovered within the Omo-Turkana Basin in the Omo Kibish Formation, dated to 220 ka (McDougall et al., 2005; Vidal et al., 2022).

1.2. Middle and Late Pleistocene archaeological research in Turkana

Following the initial discovery of KNM-ER 999 subsequent excavations near Ileret by J.W.K. Harris in 1972 revealed limited archaeological context for the fossils (Harris, 1972). Later, in 1991 and 1992, Alison Kelly (student of J.W.K. Harris) continued the Late Pleistocene research and conducted geoarchaeological survey focused on uncovering Middle Stone Age (MSA) artifact-bearing deposits. The MSA, according to Kelly (1996b), refers to a lithic technological stage in human evolution, particular to sub-Saharan Africa, characterized by prepared core technology and an emphasis on the production of points, blades, and scrapers and has been broadly associated with the appearance and evolution of *H. sapiens*.

Kelly and Harris (1992) described localities in three sub-regions of the East Turkana research area: Ileret, the Karari Ridge, and Koobi Fora Ridge. FwJi1, FwJi2, and FwJi3 were excavated near the modern town of Ileret. Near the Karari Ridge, Kelly and Harris described excavations at FxJj61 and 66 (*ibid*). GaJj17 in the Koobi Fora region was initially discovered by Charles Nelson (Kelly field notes, 1991; Nelson, personal communication). Nelson conducted a small (ca. 1 × 3 m) geological trench at the site, which was still visible upon our arrival in 2015. Alison Kelly continued research at GaJj17 in 1991 and 1992. Kelly's team conducted three 5 × 5 m surface collections and excavated a 3 × 1 m unit to 20 cm depth and uncovered 463 artifacts and 254 fossil faunal remains (Kelly, 1996a). Kelly concluded that the artifact-bearing deposit was limited to the upper 5 cm of indurated sandstone. At the time of Kelly's excavations, which lacked dateable tephra deposits, few radiometric dating options existed that could extend beyond the radiocarbon limit of ca. 45 ka; as a result, the 1991–1992 research lacked a chronological framework.

1.3. Lake level variation effects on human lifeways and archaeological interpretation

Lakes and rivers throughout the East African Rift Valley play a vital role in the lifeways of millions of people today, and the dynamic fluctuations of the present extended well into the Pleistocene. For example, Lake Victoria, the largest freshwater lake in the world, was completely dessicated from approximately 94–36 ka (Beverly et al., 2020). Lake Malawi was 200–300 m below present from ~40 to 28 ka (Finney et al., 2019). Lake Tanganyika levels were > 600 m below present prior to 25 ka (Scholz and Rosendahl, 1988). Unlike Lakes Victoria, Tanganyika, and Malawi, Lake Turkana is considered a closed-basin lake, in a predominantly arid landscape; it is the largest permanent lake desert in the world (Obiero et al., 2022). Today, while northern Kenya faces its worst drought in recorded history, Turkana lake levels are extremely high and flooding is common (Inwood, 2022).

Lake-level variation in Turkana influenced both hominin paleoenvironments and the taphonomy of paleontological and archaeological assemblages therein. Feibel (2011) described the paleogeography of the Turkana Basin throughout the Plio-Pleistocene, from the Apak floodplain, Lonyumun Lake, Moiti floodplain, Lokochot Lake, Tulu Bor floodplain, and Lorenyang Lake, the lattermost phase being associated with KNM-ER 15000. The cessation of the Omo group deposition was characterized by significant gaps in sedimentation and included the Chari Floodplain and Nachukui Lake phases, followed by the Silbo Floodplain, the last recorded fluvial system in the Omo Group (*ibid*). The formation of present-day Lake Turkana and its hydrologic variation is recorded in the Turkana Group of the Omo Kibish Formation and in the Galana Boi Formation, especially in relict beaches (Bloszies et al., 2015; Feibel, 2011). Lake levels oscillated over 30 m between ca. 14.5 and 4.5 ka (Bloszies et al., 2015) and over 50 m between ca. 8.5 and 4.5 ka (Forman et al., 2014), including a 50 m water-level fall ca. 5 ka (Garcin et al., 2012). The highly variable Holocene lake-levels were likely associated with western and eastern African monsoons and sea surface temperatures (Bloszies et al., 2015; Forman et al., 2014). During lake highstands, especially in the early Holocene, water levels exceeded 459 m asl and overflowed into the White Nile drainage system (Garcin et al., 2012), likely flooding older Late Pleistocene sites, including GaJj17, in the process.

1.4. Current Middle and Late Pleistocene research in the Turkana basin

Our research in the Turkana Basin, beginning in 2013, has focused on a multi-scalar understanding of site formation processes with an objective toward understanding how humans adapted to the dynamic environments of the Middle and Late Pleistocene in the basin. The first aim of this project was to identify archaeological sites dating to this period in primary context comprising ample sedimentary packages for excavation analysis. The GaJj17 locality provided the best opportunity to accomplish this, and we focused our initial analyses on a geological and depositional understanding of the site. This paper reports the first description of GaJj17 site evolution integrating facies analysis, micromorphology, optically stimulated luminescence dating, radiocarbon dating, zooarchaeological study, and stone artifact assemblage analysis. These site-level observations contribute to broader ongoing landscape Late Pleistocene geoarchaeological study.

2. Material and methods

2.1. Excavation

Archaeological excavation proceeded from 2016 to 2018 and focused on two primary research objectives: 1) understanding the site formational and post-depositional geological processes, and 2)

uncovering and recording the spatial information of *in situ* artifacts and fossils for archaeological interpretation. Excavations included a 2 × 2 m unit (N87E95, based on local arbitrary grid system) that extended to a maximum depth of 2 m. This area was chosen for excavation because it was located outside Kelly's 1991/1992 excavation and surface collection area and therefore was least likely to be disturbed by previous archaeological research (Fig. 2). The unconsolidated nature of the sandy deposit and high frequency of wall collapse precludes excavation larger than 2 m^2. To assess the lateral extent of the sedimentological nature of the deposit we placed an additional excavation unit (N83E87) 7 m west of N97E95, placed within the Kelly surface collection area to preserve undisturbed deposits for future research.

Our excavation procedure used a Leica Total Station laser theodolite with a Trimble handheld computer equipped with EDM-Mobile software (http://www.oldstoneage.com) (Dibble and McPherron, 1996) to piece-plot the x-y-z coordinate provenience information of all artifacts and fossils over 1.5 cm. Main Datum was marked at the same location as that used by A. Kelly using a 3m rebar pole anchor, the top of which was set with an arbitrary x-y-z provenience of 100, 100, 100. We recorded two provenience points on elongated objects to capture their orientation (bearing and plunge) following (McPherron, 2018). We sieved all sediment with a 2 mm mesh to ensure the recovery of micromammals and beads. We assigned a unique identification number denoted with barcoded labels to all piece-plotted objects. We assigned shared Lot Numbers to sieved materials, dating samples, and piece-plotted objects such that each lot corresponds to a constrained geospatial unit. Excavation units followed natural sedimentological boundaries with a maximum depth of 10 cm per lot.

2.2. Sedimentology and stratigraphy

We placed two geological trenches within the same stratigraphic horizon as the artifact-bearing deposit: GT1 and GT2. GT1 extended 1 m wide and 4.2 m long and was excavated in four steps, each of which spanned 60–70 cm height. GT2 extended 1.8 m long and 0.70 m wide. Sedimentological descriptions were done across the GaJj17 site at the geological trenches and excavation units (GT1, GT2, N83E85, N87E94). To understand the lateral extent of GaJj17 facies an additional sedimentological description was done at an archaeologically-sterile locality (NE) which showed similar outcrop features to GaJj17 and is located ca. 500 m northeast of GaJj17 (Fig. 2; Fig. 3). A sedimentary facies analysis was conducted from the sedimentological descriptions following the scheme of Miall (2014) and Feibel (2013). The facies analysis was enhanced with digital elevation data of the artifact-bearing unit recorded with a differential GPS (dGPS) using an RTK system.

We sampled sub-surface sediments for petrographic investigation (IDs 51800, 51801, 51802, 51803) from the eastern wall of N86E95 and additional samples (IDs 1711310, 1711311, 1711312, 1711313, 1711314) were taken from the northern wall of N83E85 (Fig. 2). We collected cemented sediments with a rock hammer and wrapped the sample in cling film, noting the upward direction. We sampled friable parts of the section by hammering aluminum piping into a cleared wall, carefully removing the sample from the outcrop, and wrapping with cling film.

Field collected samples were prepared for resin imbedded thin sectioning at the School of Geosciences, University of the Witwatersrand, Johannesburg, South Africa obtaining ~30 μm thin sections. We identified the mineralogy of grains following Deer et al. (1992) with an Olympus polarizing microscope. Photos of the thin section were analysed with Olympus Stream software. We analysed the thin sections under cross polarised light (XPL) and plane polarised light (PPL) to determine micromorphological features (Adams et al., 1984; Bullock et al., 1985; Goldberg, 1979; Jongerius and Rutherford, 1979; Karkanas and Goldberg, 2013; Stoops, 2003).

We conducted systematic surface collection in a 6-square-meter area (N79-82E79-81) in which all artifacts and fossils were plotted regardless of type or size. We also collected and piece-plotted surface objects at GT1, GT2, and in the immediate surrounding regions of both excavation units to prevent disturbance. All ostrich eggshell (OES), obsidian, and bone tools discovered on the surface were collected and piece-plotted for the purposes of chronometric dating, raw material sourcing, and technological analyses.

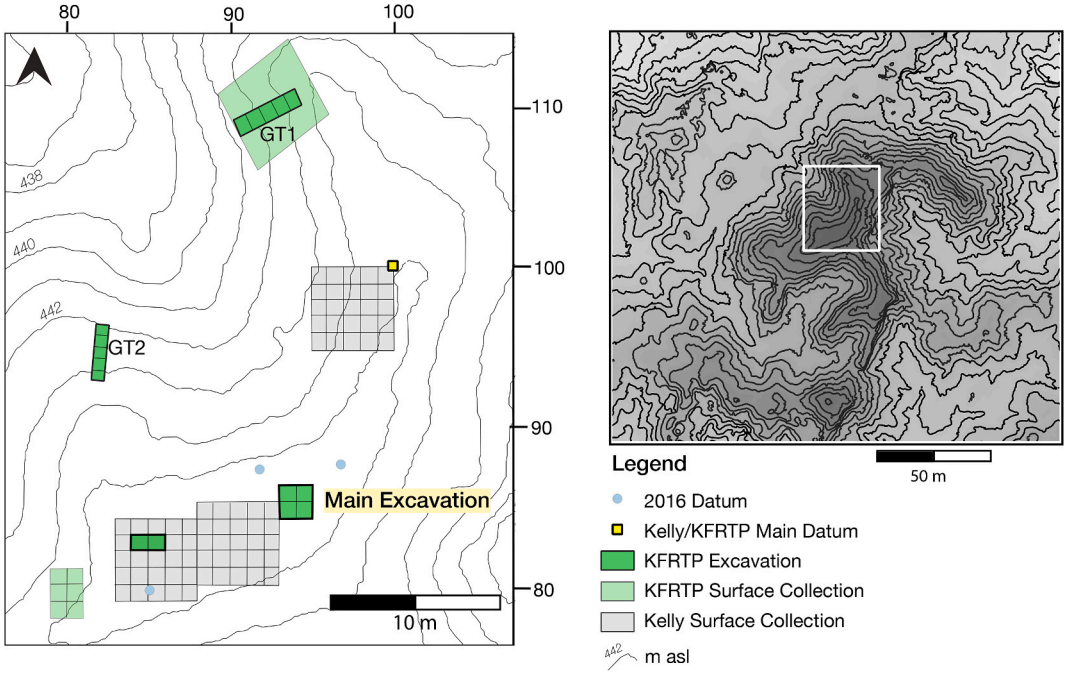

Fig. 2. Left: Plan view of the GaJj17 excavation and geotrenches showing Kelly 1991/1992 units. Right: Contour map of the GaJj17 area. White box denotes area shown on left. Note elevated nature and crescent shape of locality. m ASL = meters above sea level. KFRTP = Koobi Fora Research and Training Program.

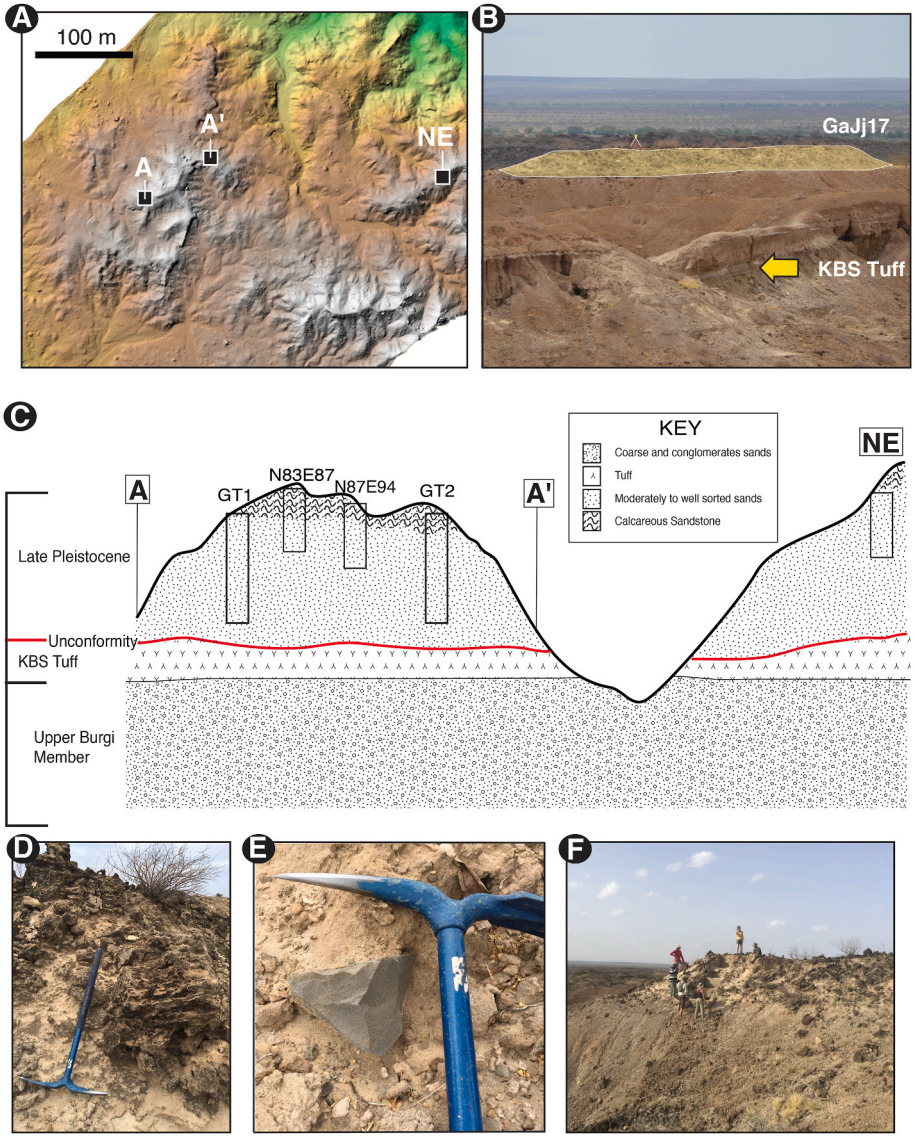

Fig. 3. Geological setting of GaJj17. A) Digital elevation model of excavation area. Imagery obtained via uncrewed aerial vehicle (UAV). B) Image of GaJj17 from the southeast, total station for scale. Late Pleistocene deposits highlighted in yellow. C) Idealized sketch (not to scale) depicting the geographic relationship of sections from GT1, N83E87, N87E94, GT2, and NE. D) Indurated sandstone which caps the site. E) Artifact eroding out of the site. Image taken in 2015 of erosional surface. F) Geotrench excavation in 2016.

2.3. Optically stimulated luminescence (OSL) dating

2.3.1. Sample collection and preparation

Five OSL samples were collected from N87E94 at 30 cm intervals down section (Fig. 4). Samples were transported in light-tight packaging and laboratory preparation was undertaken in subdued red-light conditions. Samples were rinsed in a 10% dilution of concentrated hydrochloric acid (HCl) and a 15% dilution of concentrated hydrogen peroxide (H_2O_2) to remove carbonate and organic material, respectively. The potassium (K)-rich feldspar separate was isolated via heavy liquid separation using sodium polytungstate (SPT) at a density of <2.58 g/cm^3. Samples were dried and sieved to obtain the 180–212 μm grain size fraction, which was used in all further measurements.

2.3.2. Equipment and measurement parameters

Luminescence measurements were made on individual K-feldspar grains using a Riso TL/OSL DA-20 automated reader. Optical stimulation of individual grains was undertaken with a focused 150 mW IR laser (830 nm, Bøtter-Jensen et al., 2003) fitted with a RG780 long pass filter, while simultaneous IR stimulation of all grains was undertaken by the IR LED array (870 nm, 144 mW/cm^2). Luminescence emitted in the blue region was detected by an EMI 9235QB PMT filtered by a 3 mm LOT-Oriel D410 glass filter. Laboratory irradiations were made using a ^{90}Sr/^{90}Y beta source, with a beta dose rate of 0.122 Gy/s.

Dose response curves (DRCs) were constructed using the software package Analyst (Duller, 2015) with an instrumental uncertainty of 1.5%. DRCs were fit with a single saturating exponential (SSE), double saturating exponential (DSE) or single exponential plus linear (SEPL) function to obtain the best fit. Equivalent dose (D_e) values were calculated by integrating the luminescence signals from the initial 0.15 s of the decay curve and subtracting a late background from the last 0.3 s of the decay curve. Individual equivalent dose values were only accepted if (i) the recycling ratio was within 10% of unity, (ii) recuperation was less than 5% of the natural signal, (iii) the error on the test dose signal was less than 3 standard deviations, and (iv) the uncertainty on the test dose was less than 10%. D_e uncertainty is reported as 1 standard deviation.

2.3.3. Dose rate measurements

Elemental (U, Th and K) concentrations for the bulk sediment sample were calculated using high resolution gamma spectrometry measured at VKTA laboratory in Dresden, Germany. The concentrations were converted using the conversion factors of Guérin et al. (2011) to calculate the alpha, beta and gamma dose rates for each sample. The alpha dose rate was corrected for attenuation of less-energetic alpha particles, while

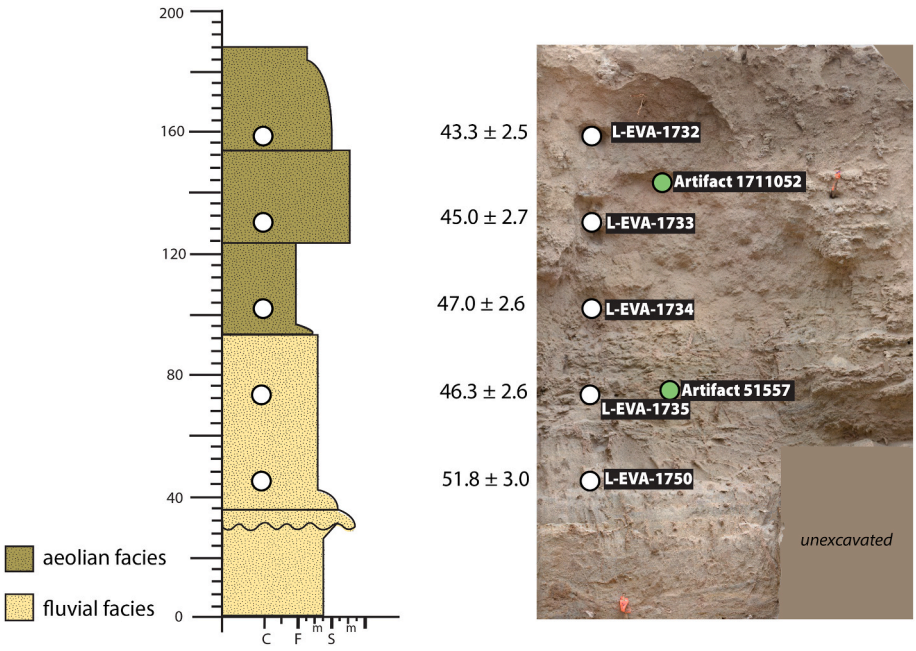

Fig. 4. Orthophoto of N profile of N87E94 with plotted provenience of OSL samples. Artifact 1711052 is illustrated in Fig. 8C and artifact 51557 is illustrated in Fig. 8A. Photogrammetric orthophoto generated using Nikon D3500 and Agisoft Metashape Professional.

the alpha, beta and gamma dose rates were corrected for grain size attenuation and water attenuation. As sedimentological results show below, the modern water content is unlikely to be representative of the burial water content, hence a burial water content of 10 ± 5% was assumed based on the measured and saturated water contents, and the unconsolidated nature of the sediments. An internal K-concentration of 12.5 ± 0.5% (Huntley and Baril, 1997) was assumed to calculate the internal beta dose rate. The contribution of rubidium (Rb) was inferred from the K-content using a ratio of 200:1 (Mejdahl, 1987). The cosmic dose rate was calculated using equation 2 of Prescott and Hutton (1994). All dose rate calculations were made using the Dose Rate and Age Calculator (DRAC, Durcan et al., 2015).

2.4. Radiocarbon dating

To better understand the age and formation of the site we collected all organic material suitable for radiocarbon (^{14}C) analysis including bone, charcoal, and ostrich eggshell. All samples analysed for radiocarbon were approved by the NMK. We tested six fossil bone samples for radiocarbon analysis, each from different contexts, including one small (0.6 g) broken fragment of a bone harpoon. Although no ostrich eggshell was found *in situ* that could be used for reliable chronological dating, several unmodified ostrich eggshell fragments were found on the surface. We dated the carbonate fraction of these OES fragments using accelerated mass spectrometry (AMS) ^{14}C analyses calibrated using the mixed IntCal/SHCal model (Hogg et al., 2020; Reimer et al., 2020) following prior analyses (Tryon et al., 2018) to create a conservative age estimate reflecting the proximity of GaJj17 to the equator, and Intertropical Convergence Zone (ITCZ; but see Nicholson, 2018).

2.5. Faunal analysis

Faunal analysis was conducted to assess the paleoenvironmental context of the site. To maximize the fossil faunal sample, all piece-plotted and sieve finds from 2016, 2017, and 2018 excavations were studied in combination with all faunal remains derived from Alison Kelly's 1991-1992 excavations. Surface and subsurface collections were analysed separately.

Piece-plotted fossils were categorized by class (*Mammalia*, *Reptilia*, *Actinopterygii*). Skeletal elements and more specific taxonomic classification were noted for each fragment whenever possible. Analysis on the sieve finds from the recent excavation were limited to element and taxon only. For all other specimens, additional measurements were noted, including the dimensions of each bone (length, width, thickness), fragment completeness (in increments of 25%), and the type of fracture (green or dry, following Villa and Mahieu (1991). All fossils were further examined for burning marks and other surface modifications (toothmarks, cutmarks, percussion marks, trampling, rodent gnawing, recent damage, and non-identifiable marks).

2.5.1. Taphonomic study of fish remains

We conducted a detailed faunal analysis of the fish remains from GaJj17 to assess a) whether the fish assemblage composition resembled that of a naturally formed or human-accumulated deposit, as differentiated by Stewart (1991) and b) whether any evidence for human consumption of fish was present (Table 1). We used different proxies to assess the nature of the assemblage: taxonomic diversity, density of remains, size bias, deviation from the natural representation of skeletal parts (cranial, axial and epaxial), and presence or absence of anthropological modifications (cut marks, percussion marks, burning). We compared the taxonomic diversity of the GaJj17 remains to that of natural land surface and human-accumulated assemblages. Following Stewart (1991), Gifford-Gonzalez et al. (1999), and Stewart and

Table 1
Summary of expected patterns for naturally and human accumulated fish bones assemblages.

Proxy	Natural assemblage	Human-accumulated assemblage
Taxonomic diversity	High (>0.63)	Low (<0.61)
Size	Greater size range	Bias towards medium size
Skeletal part proportions	Bias from differential preservation	Bias due to butchery practices
Density of remains	Low	High
Cut marks	Absent	Possible
Percussion marks	Absent	Possible
Burnt bone	Absent	Possible
Association with artifacts	No	Yes

Gifford-Gonzalez (1994) we expect a human accumulated fish assemblage to have a taxonomic diversity index between 0.42 and 0.61, which is lower than the diversity expected for natural accumulations, between 0.63 and 0.76, and which differs from the taxonomic diversity of fish in the lake (0.83); we expect only six species [*Lates niloticus* (Nile perch), *Oreochromis niloticus* (a species of tilapia), *Clarias gariepinus* (Nile catfish), *Synodontis schall* (another catfish), *Labeo horie* (a carp), and the young of *Bagrus bayad* (a deepwater catfish)] to be present, and cichlids to be overrepresented. We calculated taxonomic diversity indices using Simpson's index:

$$D = 1 - \Sigma(p_i^2)$$

where p_i is the proportion represented by the individuals in taxon *i* (Peet, 1974). We modified the taxonomic diversity indices calculated by Stewart (1991) because their study identified taxa to the genus level, while we could not identify several specimens past the family level. Our calculations use MNI, as NISP is not available for the sites studied by Gifford-Gonzalez et al. (1999).

We calculated the densities of faunal remains from GaJj17 following methodologies described in the following contexts: 1) three Holocene sites on the West shore of Lake Turkana (Prendergast and Beyin, 2018); 2) surface collections of natural deposits and modern human settlements (Gifford-Gonzalez et al., 1999; Stewart, 1991); and 3) excavations at the site of SM1, in Ethiopia (Davis, 2019). Stewart (1991) and Stewart and Gifford-Gonzalez (1994) report a fish remains density (NISP/m^2) of 0.04 for fossil natural accumulation and 0.06 for recent natural accumulation. An issue when applying these data to archaeological sites involves translating the two-dimensional density of surface collections to the three-dimensional density of archaeological excavations. Both Davis (2019) and Prendergast and Beyin (2018) used standardized densities that consider the depth of excavations. We divided the excavations in 50 cm layers and compared the densities of each following the three methods described above.

2.6. Lithic analysis

Stone artifacts were studied both as a proxy for understanding site formation and to place the lithic technology in a regional and temporal context. We analysed the lithic assemblage at the National Museum of Kenya in Nairobi, recording the raw material, tool type, technological and maximum length, technological and maximum width, technological and maximum thickness, and noting retouch, edge damage, and evidence of burning and/or heat treatment. Qualitative analysis of cores and flakes, such as flake scar patterns, platform shape and preparation (including on debordánt and overshot flakes) were recorded in notes to provide a preliminary understanding of the lithic technology(ies). We conducted size sorting analysis of the artifacts following Schick (1986). Artifact orientation analysis was done following McPherron (2018). Lithic analysis measurements followed methods used in Wilkins et al. (2017) and Pargeter et al. (2023).

3. Results

3.1. Sedimentology and stratigraphy

Stratigraphic mapping and facies analysis of local deposits indicate that GaJj17 unconformably overlies the KBS Member (Fig. 3). An angular unconformity defines the contact between GaJj17, where KBS Member beds are dipping 11° to the south and are overlain by the horizontal deposits of GaJj17. The GT sections are representative facies of the excavation and have been correlated as such (Fig. 3). Elevation data measured with dGPS indicate that the caliche at GaJj17 is located at 444.302 m above sea level (m asl). An additional locality (NE) with similar geologic characteristics is located 860 m northeast of GaJj17 and exhibits a capping caliche at 445.557 m asl and likely represents the same unit.

There are five lithofacies defined in the succession based primarily on grain size and sedimentary structures using the scheme of Miall (2014) and more specifically by the Koobi Fora Formation as described by Feibel (2013). These lithofacies are divided into three main groups as designated by grain size; gravel (G), sands (S) and fines (F).

There is a variety of facies throughout the sequence with the most diverse located in the lower-lying channel facies association unit. The sequence exhibits minimal change in color between the facies although most change is seen in abrupt lithofacies changes. Hand specimen descriptions were also limited by physical and chemical post-depositional process that affect observations. However, the detail of the sediments is preserved and newly exposed outcrop from the excavations and geotrenches conducted have allowed for thorough investigation of the sequence.

3.1.1. Lithofacies

The lithofacies are described below and shown in Fig. 5:

3.1.1.1. Gb - gravel, bedded. The facies is very distinct in the sequence and identifiable by matrix-supported moderately to poorly sorted, planar bedded sediments. The beds are usually thin averaging less than 4 cm and the sequence is also very thin (<20 cm). The facies lends its color to the variable clast lithology with a dark brown matrix. The clast shape of this conglomeratic unit are predominantly subrounded to rounded. Most clasts are pebble in size and with varied mineralogy in the form of green ignimbrite, basalt and quartzofeldspathic material and some carbonate nodule inclusion. This facies is associated with open channels in times of infrequent, high-magnitude discharge events (Miall, 2014). The clasts are sourced from in-channel and overbank (as supported by carbonate nodule inclusion) associated with adjacent soils (Feibel, 2013). The bedding in the facies indicates long-lived, sustained flows (Wilson et al., 2014).

3.1.1.2. Sl - sands, horizontally laminated. This is a common sand facies present in the sequence. Due to this common occurrence, it has variable thickness, as it forms a portion of larger sequence with associated sand facies. They are identifiable by horizontal laminae (0.5–1 cm thick) that are consistently laminated. It is a moderately to well sorted sediment with fine to very fine sands. This facies indicates super-to trans-critical upper flow regime conditions representing various part of channels. These are associated with moderate depositional rates in areas of stability where the bedforms can be deposited (Miall, 2014).

3.1.1.3. Sm - sand, massive. This facies is the most common facies in the sequence and is identifiable by a lack of sedimentary structure. The facies varies in thickness with maximum thickness of approx. 50 cm. Sorting is usually moderately to well sorted of fine to very fine sand particles. Feibel (2013) attributed this disturbance to the turbation of primary fabrics from the near-surface environment. Most of this disturbance is likely caused by bioturbation.

3.1.1.4. Fm - fines massive. This facies is identified by silt-size sediment that lacks any sedimentary structure that occurs widely in the sequence. It is characterized by medium to coarse silt grains that are moderately or well sorted. There are color variables throughout the sequence from a light to dark brown. Due to the fine grained, soft nature of the sediment it is very friable; this makes for rapid physical weathering and poor exposure.

This facies is associated with crevasse splay deposits (in upward fining sequences) indicating waterlogged overflow from rapid flows that are waning, which leads to lack of structure, and representing high water content, specifically a high-water table in a floodplain (Miall, 2014; Wilson et al., 2014).

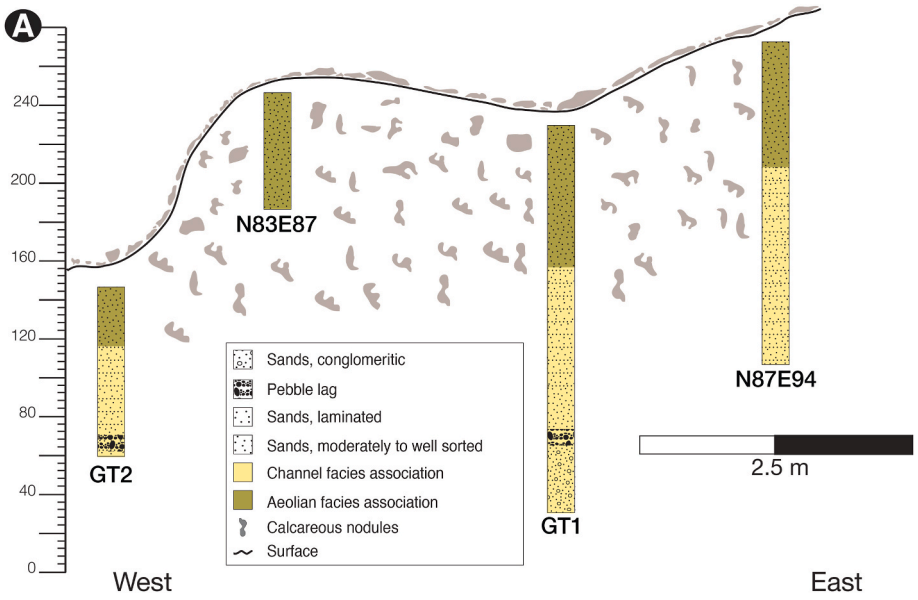

Fig. 5. Stratigraphy of GaJj17.

3.1.1.5. Fl - fines, laminated. This facies is identifiable by medium to silt-to clay sized horizontally laminated, well sorted sediments. It contains medium to fine grains that are usually well sorted. Each horizontal laminate is approximately 0.3 cm thick. The facies indicates sediments that are suspended on a planar surface. This occurs in currents that lack energy required to transport sediment. This forms part of the short-lived ponds on floodplains as seen with the suspension settling (Miall, 2014) which has a close association with the water table intersecting the surface.

3.1.2. Facies association

These five lithofacies have been grouped into three lithofacies associations with some overlap in the occurrence of facies (Table 2). These lithofacies associations represent paleodepositional environmental interpretations.

3.1.2.1. Fl_f - floodplain. The floodplain facies association is the fine-grained fluvial facies association represented by mostly siltstone and mudstone facies. Lamination (Fl) is the most common sedimentary structure although there is usually no sedimentary structures present (Fm). The facies association demonstrate some bioturbation (rhizoliths and burrowing). This facies association is usually transitioned with the other fluvial facies association. This transition here is stepwise as seen by repeated distinct stratigraphic particle changes (sands to muds) reflecting a more long-lived change in environment and energy loss. The brown colouring of mudstones can be attributed to high organic matter present (Smith et al., 2008).

3.1.2.2. Fl_c - fluvial, channel. The fluvial channel facies is defined by a base characterized by erosion with scour fill (typically about 10 cm thick). These scour surfaces are filled with gravel lags with pebble sized particles (mostly representing Gm facies). This can happen consistently for a few beds but usually grade into thicker, finer grained sand facies arranged in a larger upward fining succession. The most distinct of these sand facies are Sm and Sl. In addition, the facies association can have truncation in a sequence which is overlain by the same sequence described. There are overbank flows of fines present in the form of silts. The lag deposits are usually overlain localized (small-scale) lamination.

3.1.2.3. A_w - aeolian, wind-blown. This is a thick unit from the upper part of the sequence. It is represented by homogenous sands that are moderately sorted. The petrographic analysis mimics the texture observed in the section (Fig. 6B). The unit is sandy, consisting mostly of quartz (monocrystalline) with some feldspars (present in the form of albite and microcline) and some lithic fragments as biotite and chlorite. The grains are subangular to angular and non-spherical (Fig. 6B). The unit is clast-supported with no interstitial material.

Table 2
Facies associations of GaJj17.

Facies Associations	Lithofacies
Fl_f - Floodplain	Fm, Fl
Fl_c - Fluvial, channel	Gb, Sl, Sl
A_w - Aeolian, wind-blown	Sm, Sl (convoluted)

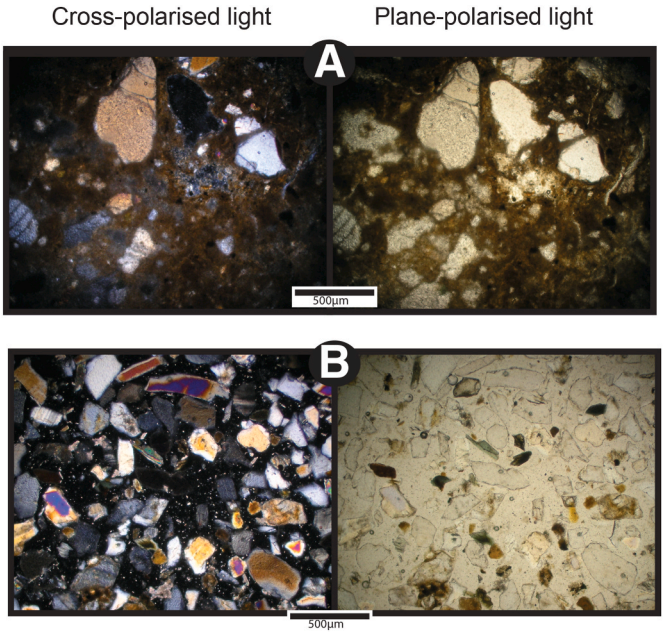

Fig. 6. Photomicrograph of aeolian blown sands in the upper part of the sequence showing (A) cementation of grains which create a caliche and (B) surrounding uncalcified section showing moderately sorted sands with angular to subanglar grains. *(single column width)*.

The sandy unit is associated with indurated (poorly sorted) calcareous nodule characteristic of caliche. Microscopically, the nodules comprise polymictic angular to subangular grains (Fig. 6A). The mineralogy is like that mentioned above but includes polycrystalline quartz grains. It is also matrix supported and contains calcite as interstitial material cementation.

The facies associated with this deposit are Sm with some convoluted lamination present. The consistent grain size with good sorting suggests wind transport. The lack of sedimentary structures (Sm) and the disturbed laminations can be attributed to bioturbation or other post depositional disturbances like calcification.

3.2. Geochronology

3.2.1. OSL dating

3.2.1.1. Equivalent dose measurements. Initial tests on the OSL signal from quartz were hampered by a dominant infrared stimulated luminescence (IRSL) signal from feldspar inclusions within the quartz grains. Attempts to measure the post-IR OSL signal produced decay curves with low signal intensity dominated by either 1) a blue-stimulated feldspar OSL signal (Thomsen et al., 2008) or 2) a medium or slow component in the blue-stimulated quartz OSL signal (Singarayer and Bailey, 2003). Therefore equivalent dose (D_e) measurements were made on K-rich feldspar grains using the post-infrared infrared stimulated luminescence (post-IR IRSL) technique at an elevated stimulation temperature of 225 °C using the modified protocol of Colarossi et al. (2018) with a test dose of 30 Gy. Suitability of the protocol to these samples was assessed using a dose recovery test. Grains were bleached in a UVA Cube 400 solar simulator for 4 h. A residual signal of 5.09 ± 0.29 Gy (n = 74) was measured from two single-grain discs. An additional three discs were irradiated with a 122 Gy beta dose, the D_e values were measured, and the residual subtracted. A measured/given dose ratio of 1.02 ± 0.01 (n = 135) was calculated for sample L-EVA-1734 (acceptable results fall within the range 0.90–1.10). For natural D_e measurements at least three discs were measured per sample, with ~35% of the measured grains passing the acceptance criteria (see Section 2.3.2 and Table 3). The individual K-feldspar grains produced bright luminescence signals with well-defined dose response curves and minimal sensitivity change during measurement (Fig. 7a-b).

The natural D_e distributions are similar for all samples (Fig. 7C), with overdispersion (OD) ranging from 32 to 37% and mean D_e values of ~115 Gy. Low OD (4%) measured during the dose recovery test implies most of the variation observed in the natural D_e distributions is likely

Table 3
Analysis data for single grain equivalent dose measurements.

Sample ID	L-EVA-1732	L-EVA-1733	L-EVA-1734	L-EVA-1735	L-EVA-1750
Total number of grains measured	300	300	300	300	300
Signal indistinguishable from BG level	91	128	113	137	65
Grains producing a dose response curve	209	172	187	163	235
Number of saturated grains	0	0	1	1	0
Grains that failed acceptance criteria:	**82**	**78**	**74**	**70**	**103**
Recycling >10%	22	23	21	8	35
Recuperation >5% of the Natural signal	15	14	10	15	17
Maximum test dose error >10%	45	41	42	47	48
Excessive sensitivity change mid-sequence	0	0	1	0	3
Number of grains in ED distribution	**127**	**94**	**112**	**92**	**132**

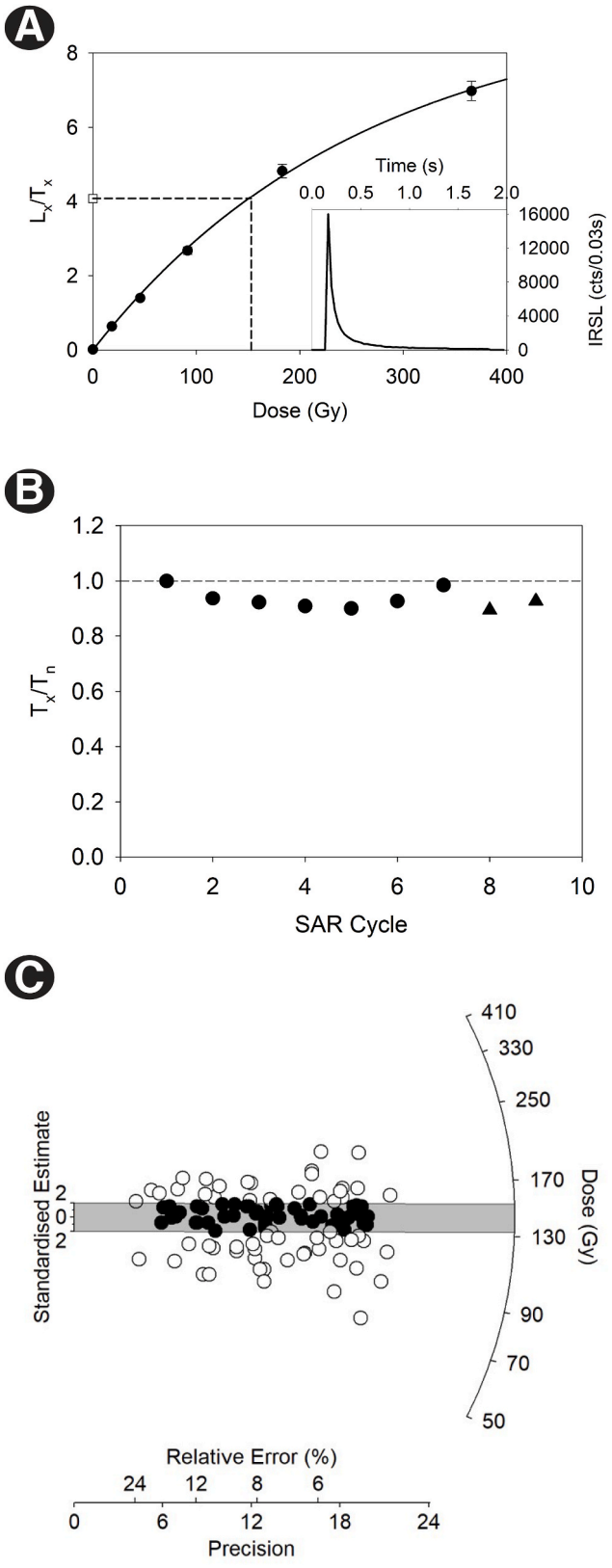

Fig. 7. A) A typical dose response curve for a single grain of K-feldspar from sample L-EVA-1734, inset shows the natural signal for the same grain. B) the T_x/T_n plot recording the amount of sensitivity change during the post-IR IRSL measurement cycle. C) The D_e distribution for the same sample (n = 112) shown as a radial plot (Galbraith, 1990), the grey bar denotes the 2σ region around the Average Dose Model (ADM) D_e value of 143 ± 4 Gy. Shaded datapoints fall within the 2σ region.

due to extrinsic factors (i.e., the depositional environment). Partial bleaching is generally not considered a major source of OD in aeolian environments (e.g., Carr et al., 2016; Lomax et al., 2007). Furthermore, the OD values reported for samples in this study are comparable to values reported for well-bleached single grain post-IR IRSL D_e distributions (e.g., 21% (Reimann et al., 2012), 37% (Carr et al., 2019). More likely potential sources of OD in the Koobi Fora region include beta dose rate heterogeneity (e.g., Mayya et al., 2006; Smedley et al., 2020), variable K content in feldspar grains (e.g., Smedley et al., 2012), and post-depositional mixing (e.g., Carr et al., 2016) given the broad distributions and lack of an obvious leading edge (Fig. 7C). Therefore, the reported ages were derived using the Average Dose Model (ADM) of Guérin et al. (2017).

3.2.1.2. OSL age calculation. The OSL ages (Table 4) range from 43.3 ± 2.5 ka to 51.8 ± 3.0 ka and appear to increase with depth, with the exception of L-EVA-1735. However, when considered by facies, the ages are stratigraphically consistent (Fig. 4), with the upper aeolian facies ages ranging from 43.3 ± 2.5 ka to 47.0 ± 2.6 ka, and the lower fluvial facies ages ranging from 46.3 ± 2.6 ka to 51.8 ± 3.0 ka. Furthermore, when considering the associated errors, the uppermost 4 ages are indistinguishable from one another. Such overlapping ages have been reported for dune environments previously by Burrough et al. (2007), Lomax et al. (2011), and Thomas and Shaw (2002). The overlap makes it difficult to separate distinct depositional events in broad-scale OSL studies and nearly impossible in a small-scale study such as this.

3.2.1.3. Fading measurements. Fading measurements were undertaken on two samples using the procedure described by Huntley and Lamothe (2001) with the preheat step completed directly after irradiation and prior to storage as per Auclair et al. (2003) and a maximum delay period of 78 days. Mean g-values of 2.09 ± 0.43%/decade and 2.05 ± 0.52%/decade were measured for samples L-EVA-1734 and L-EVA-1750, respectively. Low g-values have been interpreted as laboratory artifacts (Thiel et al., 2011), therefore fading of the natural signal is negligible in nature and fading corrections were not applied to these samples.

3.2.2. Radiocarbon dating

We generated one AMS ^{14}C date from surface OES (Table 5). Of the six fossil bone samples tested for radiocarbon analysis, all failed the initial %Nitrogen testing. Three samples contained 0.00% N, two gave a result of 0.01% N, and one 0.03% N. The threshold needed for radiocarbon analysis is 0.5% N; thus, the GaJj17 bone samples failed dramatically indicating their extremely poorly preserved nature. No charcoal was retrieved.

3.3. Site formation and paleoenvironmental reconstruction

We excavated ca. 10 m^3 area (Fig. 2) resulting in 321 piece-plotted artifacts and fossils. 106 artifacts and 66 fossils were piece-plotted and collected from the surface. In GT1 85 artifacts and fossils were discovered derived from a thin (7–8 cm) layer of consolidated orange sands in association with a pebble conglomerate. Excavations in 2016, 2017, and 2018 included units N83E85 (2 × 1 m) and N87E94 (2 × 2 m, also called Main Excavation). We used sandbags to support the excavation walls in between field research seasons. Main excavation exposed the largest surface area of the deposit enabling detailed sedimentological analysis. Stone artifacts were recorded predominantly in the upper 50 cm of the deposit, like results reported by Kelly and Harris (1992).

Table 5
Radiocarbon (^{14}C) date from GaJj17. Measured from the carbonate fraction of ostrich eggshell, calibrated using Calib v.8.2 software (Stuiver and Reimer, 1993) and a mixed SHCal20 and IntCal20 calibration curve with equal contributions (Hogg et al., 2020; Reimer et al., 2020).

Context	Laboratory Code	^{14}C yr BP (±1σ)	calBP (95.4%)
Surface	UBA-40187	2806 ± 24	2785–2960

3.3.1. Stone artifact analysis

The lithic technology at the site (Table 6) trends toward smaller (<4 cm) stone tools on a diverse array of raw materials, including cryptocrystalline silica (CCS), basalt, and quartz. Preliminary lithic analysis on both surface and excavated artifacts indicates the presence of preferential bifacial hierarchical core technologies (Shea, 2020; see also Boëda, 1995) on both CCS and volcanic raw materials (Fig. 8). The co-occurrence of objects like points and blades on various raw materials align these tools with the African Middle Stone Age (McBrearty and Brooks, 2000; Shea, 2020; Shea and Hildebrand, 2010; Tryon and Faith,

Table 6
Lithic artifact assemblage description. CCS = cryptocrystalline silica and includes jasper, chert, and similar materials. Volcanic category includes basalt and ignimbrite. Obsidian pieces are highlighted separately here.

		Count
Raw Material		
	CCS	314
	obsidian	5
	quartzite	6
	volcanic	194
Completeness		
	complete	227
	fragment	297
Tool type		
	blade/bladelet	26
	core	29
	flake	454
	grinding stone	1
	hammerstone/minimal core	2
	point	12

Table 4
Summary of OSL results.

Sample ID	Dose rate							Equivalent dose			
	Modern WC (%)	Saturation WC (%)	U (ppm)	Th (ppm)	K (%)	Cosmic dose rate (Gy/ka)	Environmental dose rate (Gy/ka)	n	OD (%)	D_e (Gy)	Age (ka)
L-EVA-1732	0.3	25.7	0.74 ± 0.18	1.63 ± 0.14	2.04 ± 0.14	0.22 ± 0.02	3.14 ± 0.15	127	33	136 ± 4	43.3 ± 2.5
L-EVA-1733	1.2	24.7	0.77 ± 0.20	2.01 ± 0.15	2.06 ± 0.13	0.20 ± 0.02	3.16 ± 0.15	94	37	142 ± 5	45.0 ± 2.7
L-EVA-1734	0.9	26.9	0.72 ± 0.21	1.73 ± 0.13	1.99 ± 0.13	0.18 ± 0.02	3.05 ± 0.15	112	32	143 ± 4	47.0 ± 2.6
L-EVA-1735	2.6	28.9	0.71 ± 0.18	2.40 ± 0.20	1.77 ± 0.12	0.18 ± 0.02	2.90 ± 0.14	92	33	134 ± 4	46.3 ± 2.6
L-EVA-1750	1.0	29.4	0.56 ± 0.15	1.62 ± 0.14	1.95 ± 0.15	0.17 ± 0.02	2.96 ± 0.15	132	32	153 ± 4	51.8 ± 3.0

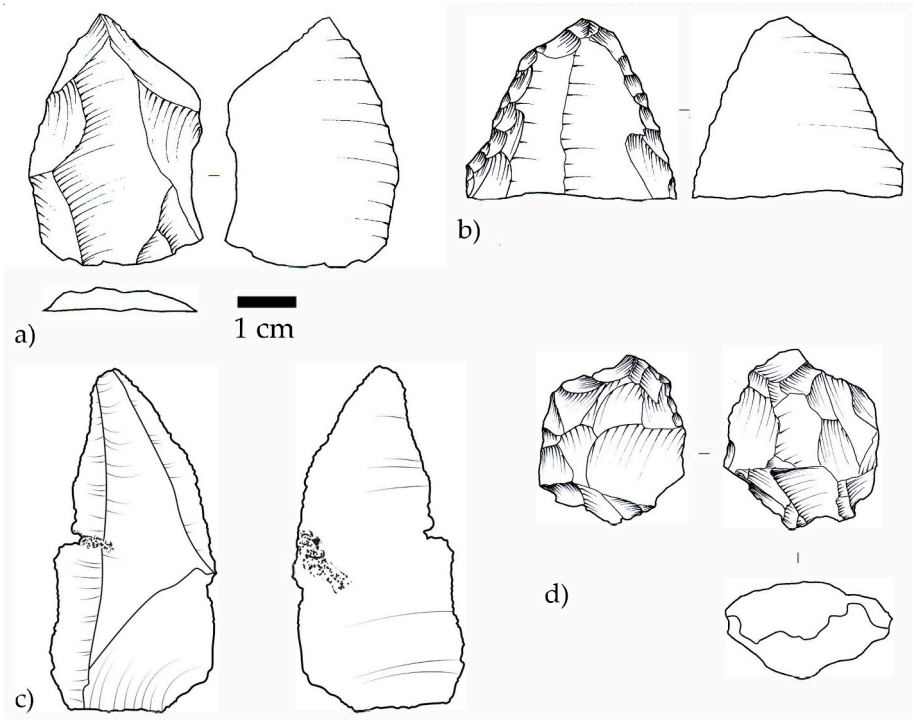

Fig. 8. Stone artifact examples from GaJj17, illustrated in Adobe Illustrator following the STIVA method (Cerasoni, 2021): A and C) triangular flakes associated with bifacial hierarchical cores (VI.C.3; Shea, 2020) (CCS), B) distal point fragment with edge damage (CCS), D) radial core (CCS). All artifacts except for D from sub-surface context and recorded with total station.

2016; Will et al., 2014).

Size sorting of the excavated finds indicates likely winnowing from fluvial action (Fig. 9A). Fig. 9B shows the relative abundance of artifacts and fossils relative to depth, indicating an increased abundance in the frequency of finds between 30 and 40 cm below the surface. Fig. 9C–E demonstrates artifact orientation data following McPherron (2018): the plunge and plano-linear orientation of finds could indicate some settling from fluvial movement.

3.3.2. *Faunal analysis*

With few exceptions, the bones are highly fragmentary, with most being broken, embedded in a matrix, and/or rolled to some extent. A total of 1306 fragments could be identified to class: 893 were fish (68.4% of total assemblage), 381 were mammalian (29.2%), and 32 were reptile (2.5%) (Table 7). Siluriform cranial fragments were the most abundant identifiable specimen to order due to their characteristic appearance. The mammal fossils of the excavation notably contain a

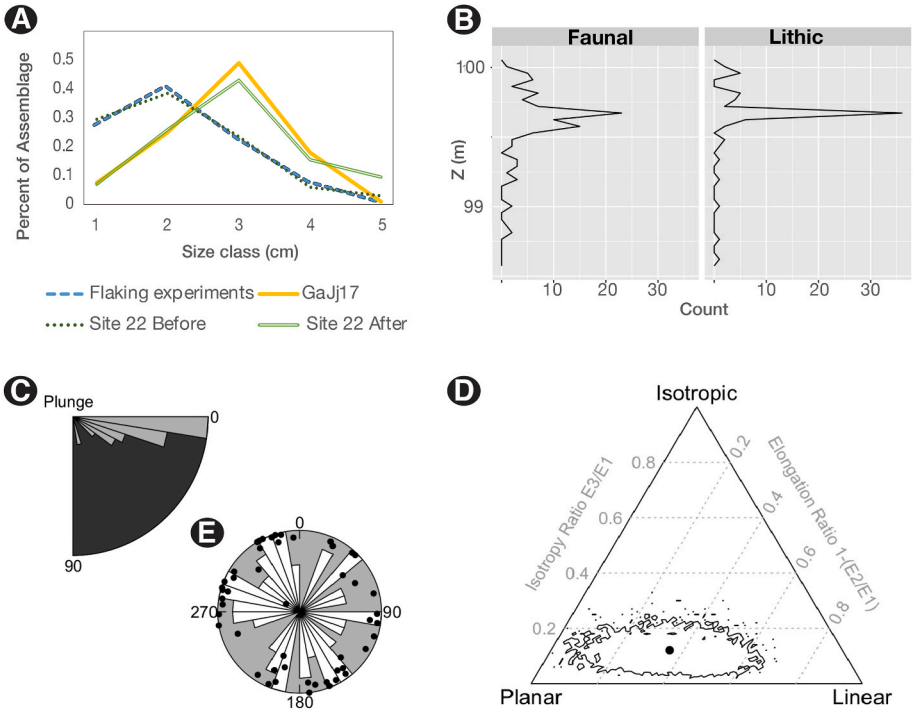

Fig. 9. A) Size distribution of stone artifacts from GaJj17 relative to experimental sites described in Schick (1986) (size class 1 = 0–1 cm, size class 2 = 1–2 cm, size class 3 = 2–4 cm, size class 4 = 4–8 cm, size class 5 = 8–16 cm). Flaking experiments from Schick (1986):27 Table 3.1 (total proportion). Site 22 refers to Schick's experimental site located on a channel bank at Koobi Fora. Before: distribution when Schick placed objects for experiment. After: 20 months later following localized flooding. B) Frequency of faunal and lithic finds relative to depth of excavation; y axis in m in relation to Main Datum at the surface (100, 100, 100; Fig. 2); height (z) was measured with a total station following Dibble and McPherron (1996). C-E) Analyses of two-shot archaeological orientations using R source code in McPherron (2018).

Table 7
Distribution of faunal remains from GaJj17 per taxon.

Taxon	Subsurface		Surface		Total	
	NISP	%	NISP	%	NISP	%
Mammalia	**41**	**10.4**	**97**	**39.4**	**138**	**21.6**
Oryx beisa	1	0.3		0.0	1	0.2
Bovidae sp.	1	0.3	1	0.4	2	0.3
Hippopotamus amphibius	1	0.3	16	6.5	17	2.7
Micromammal	1	0.3			1	
Mammalia sp.	37	9.4	80	32.5	117	18.3
Reptilia	**12**	**3.0**	**15**	**6.1**	**27**	**4.2**
Crocodylus sp.	9	2.3	12	4.9	21	3.3
Trionyx triunguis	2	0.5	1	0.4	3	0.5
Testudines sp.	1	0.3	2	0.8	3	0.5
Actinopterygii	**341**	**86.5**	**134**	**54.5**	**475**	**74.2**
Cichlidae sp.	31	7.9	12	4.9	43	6.7
Latidae sp.	12	3.0	1	0.4	13	2.0
Perciformes sp.	24	6.1	6	2.4	30	4.7
Clariidae sp.	121	30.7	53	21.5	174	27.2
Siluriformes other[a]	6	1.5			6	0.9
Siluriformes sp.	12	3.0	11	4.5	23	3.6
Tetraodon lineatus	2	0.5	3	1.2	5	0.8
Labeobarbus sp.	2	0.5			2	0.3
Actinopterygii indet.	131	33.2	48	19.5	179	28.0
Total	**394**	**100**	**246**	**100**	**640**	**100**

[a] Due to the available comparative materials, some Siluriform remains could only be identified as non-Clariidae, with family otherwise unspecified.

mixture of terrestrial and semi-aquatic species. They include a *Phacochoerus* sp. unerupted dental pillar; a partial right maxilla with the second premolar intact belonging to *Oryx beisa*, an unspecified distal phalanx; one femur shaft belonging to a micromammal, and multiple *Hippopotamus amphibius* teeth and bone fragments, including one cuboid, one metapodial, two intermediate phalanges, and many dental fragments consisting of broken tusk, partial post-canines, and enamel fragments. The reptile fossils were extremely fragmentary and rolled. We identified several *Crocodylus* teeth and one osteoderm, one phalanx from *Trionyx triunguis*, one testudine vertebra and two plastron or carapace fragments.

Of the fragments mentioned above, 431 came from surface collections and yielded an NISP of 246. Of them, 134 were from ray-finned fish, with all major skeletal elements represented broadly; crania, teeth, vertebrae, dorsal spines, and ribs were all present. Surface fossils may not be ecologically associated with the excavated specimens described above. Fifteen fragments belong to reptiles, with only one further identifiable: a partial *Crocodylus* tooth. These specimens include a partial vertebra, a proximal phalanx, and multiple tusk fragments.

3.3.3. Fish analysis

Generally, the fish assemblage was very fragmentary and not well preserved (Fig. 10). A greater proportion of the identifiable remains from the subsurface (*in situ)* materials are fish (77.4%) than in the case of surface finds (51.7%). Reptile remains are even scarcer *in situ* (1.5% vs. 4.4%). Mammals also represent a smaller proportion *in situ* relative to the surface (21.1% vs. 44.6%). Surface materials were examined separately from the rest of the assemblage. This analysis focuses on the *in situ* finds.

In our taphonomic analysis of the fish assemblage, different lines of evidence lead to somewhat divergent conclusions (Table 8). No anthropogenic or carnivore bone surface modifications were observed on any fragment, regardless of class. No bones showed signs of burning. The lack of anthropogenic modifications, which are very difficult to identify (Archer and Braun, 2013; Willis et al., 2008) and very high taxonomic diversity are in line with estimates of natural accumulations. On the contrary, the very high density of faunal remains suggests that they may have accumulated during one—or multiple—human occupations at the site. In all three analyses the density of faunal remains from GaJj17 is particularly high in the first 50 cm, and in the subsequent 50 cm (Supplemental Table 1). The size data showed a bias toward medium size, which is within the size range of fish captured by humans today at Turkana. The data for skeletal part proportions yields ambiguous results. If the epaxial elements are included when compared to data from natural accumulations, GaJj17 data suggest a deviation from natural skeletal part proportions and could possibly indicate butchery practices; however, if epaxial elements are removed, then there is no obvious deviation from the skeletal part proportions of natural accumulations for Siluriformes. For Perciformes, the cranial-to-axial ratio could indicate human butchering activities.

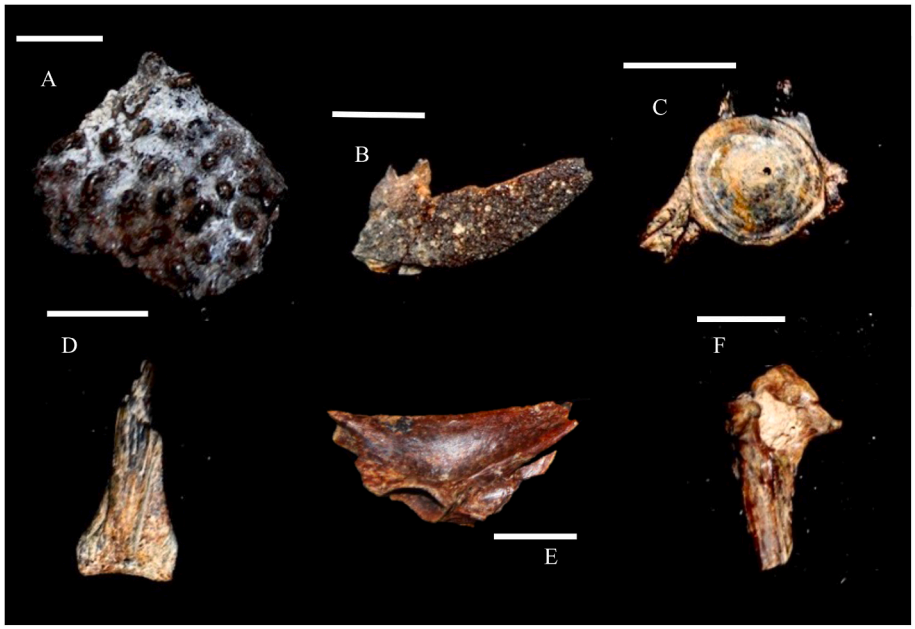

Fig. 10. Clariidae neurocranium fragment (A); Clariidae prevomer (B); Cichlidae precaudal vertebra (C); Latidae dorsal spine (D); Clariidae operculum (E); Perciform pectoral spine (F). Scale = 1 cm.

Table 8
Summary of GaJj17 fish assemblage.

Proxy	GaJj17	Indicative of natural- or human-accumulation
Taxonomic diversity	High (0.8)	Natural
Size	Bias toward medium size	Human
Skeletal part proportions	Overrepresentation of epaxial elements	Human?
Density of remains	High	Human
Cut marks	Absent	Natural
Percussion marks	Absent	Natural
Burnt bone	Absent	Natural
Association with artifacts	Yes	Human

4. Discussion

4.1. Summary of GaJj17 geoarchaeology

Our investigations at GaJj17 revealed evidence for the presence of humans in the region 43.3 ± 2.5 to 51.8 ± 3.0 ka. The site underwent a series of different depositional regimes. The ages reported here derive largely from aeolian depositional regimes with one age derived from a fluvial regime. These ages represent only a sample of the deposits studied here; continued geochronological work at similar localities and older sediments, along with refined sedimentological analyses, are ongoing to understand these findings in broader landscape context. Post-depositional processes, most notably caliche formation, cemented the deposit, thereby protecting it during lake level variation throughout the Holocene. The formation of caliche incorporated stone artifacts and fossils and is currently invariably eroding, leaving behind a palimpsest of Late Pleistocene and Holocene surface archaeology. Micromorphology and sedimentological evidence indicate that the sub-surface deposit is in primary context. Artifacts associated with Late Pleistocene humans elsewhere in eastern Africa (see Shea, 2020) are associated with the OSL samples (Fig. 4). The sharp edges of these stone artifacts

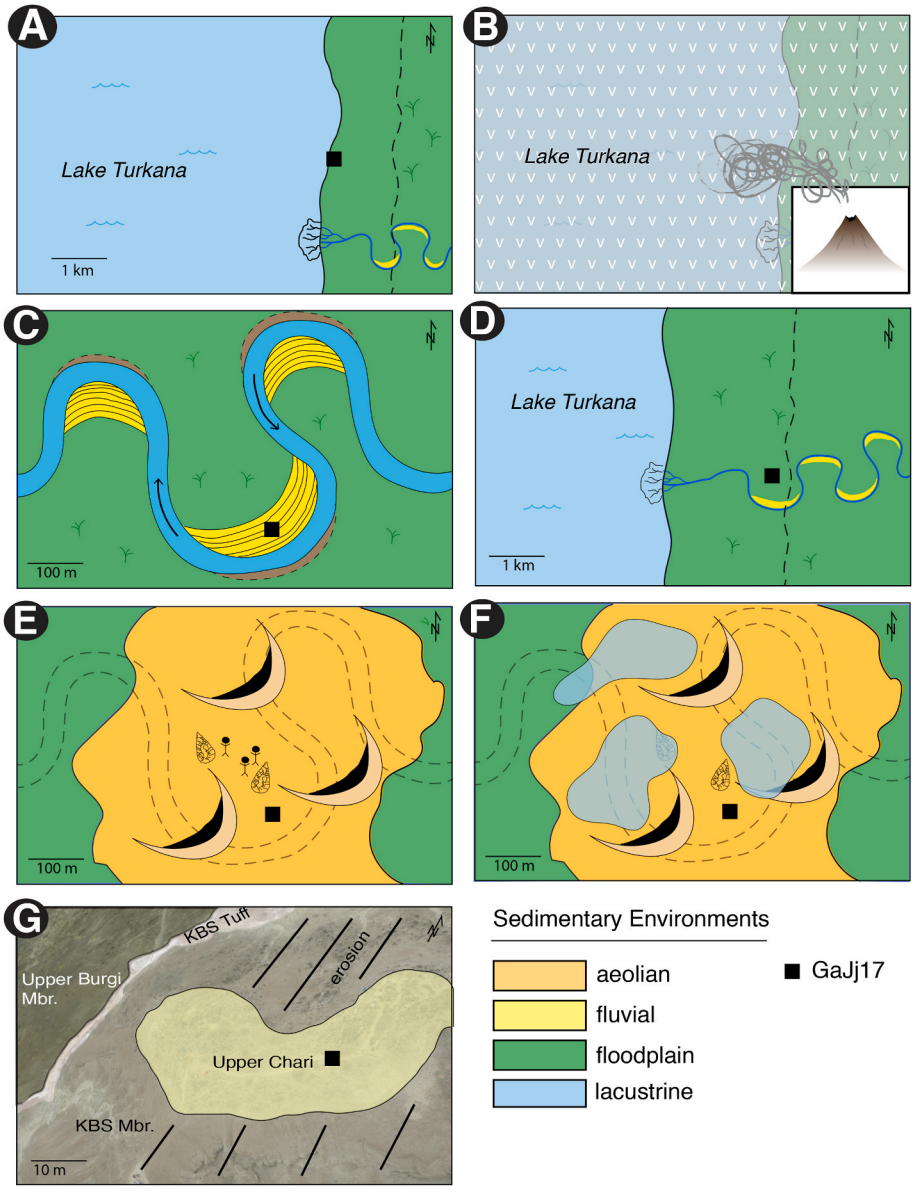

Fig. 11. Depositional evolution timeline of GaJj17. A) (2.1 Ma) Low topography; dominated by a large lake; highly sinuous rivers on floodplains feed the lake at deltas; fluctuations of lake water volume cause changes in lake level, resulting in transgressive and regressive shorelines (Feibel, 2011). B) (1.86 Ma) Volcanic eruption; ash is deposited forming the KBS tuff (Feibel, 2011). C) (1.86 Ma) Low topography; highly fluctuating lake due to quick lake water volume changes; large transgressive and regressive shorelines; highly sinuous rivers on floodplains feed the lake at deltas (Feibel, 2011). D) (53 Ka) Low topography; lake shoreline is 3–5 km to the west; highly sinuous rivers on the floodplain deposit sediment on pointbars; erosion of the floodplain occurs at the cut bank (facies Fl_r. E) (49 Ka) Sand dunes migrate over floodplain and fluvial channels; lake shoreline is 3–5 km to the west (facies Fl_c); Middle Stone Age occupation leaves associated artifacts in eolian deposits (facies A_w). F) (46 Ka) Ground water table rises and caliche lithifies artifacts with eolian deposits. G) (~10 Ka - present) Holocene occupation leaves associated artifacts on surface of lithified archaeological deposits; considerable erosion leaves behind only an isolated deposit with *in situ* stone artifacts.

coupled with orientation analysis (Fig. 9) further establish their association with the sub-surface deposit and OSL ages. Some degree of winnowing affected the archaeological assemblage which we posit may be characteristic of Late Pleistocene localities near the eastern shores of Lake Turkana. The relatively low density of artifacts and fossil fauna is also seen in other regions with complex aeolian depositional histories, such as the Western Cape of South Africa, and highlights the need for continued landscape-scale archaeological study especially work that increases excavated volume across space (Braun et al., 2013). The location of the site, coupled with abundant aquatic taxa, suggest humans utilized lakeside or near-shore environments, suggesting a need for continued zooarchaeological research in this time period and region.

4.1.1. GaJj17 site evolution

We provide a five-phase simplified model for understanding the evolution of GaJj17. We note that the model described here began sometime post-Early Pleistocene, marked by a substantial unconformity, although the precise initiation point is currently unknown. Phase 1) Low-energy fluvial transport of massive sands and polymictic conglomerate, Phase 2) Aeolian formation of dune field during time of low-lake stand, Phase 3) Late Pleistocene site occupation by humans and further accumulation of aeolian-transported sand, Phase 4) Gradual formation of caliche via percolation of groundwater, Phase 5) Holocene occupation by fisher-pastoralists, high-lake stand inundation erodes surrounding region; irregular dissolution of caliche at less-calcified points (Fig. 11). We emphasize the simplified nature of this model and the possibility that the phases outlined above may have overlapped, rather than occurring as distinct phases. Additional sedimentological characterization is needed at other localities to better calibrate and understand the evolution of this landscape throughout the later Pleistocene (see Fig. 11).

Comprehensively, our results suggest that GaJj17 represents the remnant of a paleosurface that was formed predominantly by aeolian processes during an extensively erosive time (see: McLaren, 2011). The erosional forces occurred predominantly during what we call Phase 1 via medium to high-energy fluvial processes as evidenced by upward-fining sequences with conglomeritic units and massive sands (Miall, 1996). During Phase 2, a time of low-lake stand, nearby sandy lacustrine beach deposits were exposed. Winds likely originating from the lake carried these sands in a predominantly easterly direction, forming the crescent shaped lunate landform seen today (Pye and Tsoar, 2008, 236); these aeolian processes varied with local climate conditions including wind direction and vegetation. As a result, repeated saltation and deflation of sediments was likely. We predict that the aeolian formation and ongoing deflation of the dune likely occurred over the span of several tens of thousands of years, but this remains to be further verified with additional fieldwork focused on landscape scale sedimentological descriptions. While this reconstruction is based on observed facies associations and micromorphological work we emphasize that the observed feature is an erosional remnant shaped by many processes and more research on aeolian deposition in the Turkana Basin is needed.

Based on the presence of sharp-edged artifacts and fresh fossils (weathering stage 2, Behrensmeyer, 1978) in the upper ~ 50 cm portions of this primary sandy deposit, it is likely that stone artifact discard (Phase 3) occurred during the time when the aeolian deposit was still forming. The unit comprises a sandy, unconsolidated loose sediment thus there was vertical movement of sand grains and to some extent, fossils and artifacts (Cahen and Moeyersons, 1977). As a result, at this junction we refrain from drawing conclusions that rely on a strict depositional relationship between fossils and artifacts. As demonstrated through the facies analysis and petrography describing syn- and post-depositional processes this site today can confidently be regarded as being in its primary context. The OSL evidence indicates that the sands were deposited between 52 and 43 ka.

During Phase 4, an increase in lake level increased the localized water table, likely providing the groundwater that formed the caliche deposit; no pedogenic features were observed in the aeolian sands though pedogenic calcrete formation sourced from underlying facies may have also been possible. The post-depositional incorporation of artifacts and fossils into the sandstone explains why the density of these objects is much higher in the caliche relative to underlying sands as observed in both Kelly's 1991/1992 excavations and in the excavations described here. The artifacts and fossils found in the horizon can be considered as part of the syn-depositional formation of the primary sedimentary package under investigation. The caliche observed in the package is a post-depositional feature and represents the presence of near-stagnant water in the primary deposit, such as that of a phreatic zone, which we considered in the OSL burial water content calculation. This phreatic activity can only occur if there is already a host sediment present and has limited energy thus minimal particle transportation can occur. Considering this depositional history, the artifacts found can be regarded as *in situ*, minimally affected by the near-stagnant phreatic water that later caused the caliche to form. In addition, the lack of pebble-sized clasts equal to those of the artifacts eliminated the possibility of hydraulic deposition of these tools. There is also a lack of overlying Holocene sediment lithology (unconsolidated reddish fine-grained sands and fines of the Galana Boi Formation) in the artifact-bearing horizon, which would have alluded to scouring and percolation for an introduction of more recent artifacts to the sedimentary package.

The fifth and final phase is characterized by continuous lake level fluctuation throughout the Holocene, including high lake stands which may have submerged GaJj17 which sits approximately 440 m asl (Fig. 2). During this time of extensive lake-level fluctuation, the indurated caliche deposit likely buffered the underlying artifact- and fossil-bearing sands from erosive cycles that would have taken place when lake levels receded. The irregular nature of the caliche is likely due to variations in calcification. GaJj17 represents the remaining *in situ* sandstone. In places where the sandstone eroded fully, however, the underlying sandy unit became exposed and was subsequently eroded during rapid lake transgressions and regressions of the Holocene. Although Galana Boi sands are no longer present at the site we posit that the site was re-inhabited by fisher-foragers, possibly fisher-forager-pastoralists (Beyin et al., 2017; Prendergast and Beyin, 2018) based on the presence of a surface fossil bone harpoon dated to 2785–2960 cal BP (Table 5). We report this age to underline the necessity of considering both site formation and erosional processes in interpreting behavioral conclusions from biocultural archaeological remains. This direct date also underscores the palimpsest nature of the surface collection and the necessity of ruling out depositional mixing before drawing behavioral conclusions that imply sedimentological association.

Future work at and around GaJj17 is needed, including structural geological work. Stratigraphic understanding within a tephra stratigraphic framework will also be beneficial and is underway. GaJj17 represents the first dated Late Pleistocene occurrence of human occupation in the Lake Turkana region and the only currently known Late Pleistocene locality within the Koobi Fora region. Our surveys of the surrounding area yielded no evidence for additional primary deposits similar to GaJj17. It is possible that the general lack of similar deposits near Koobi Fora is related to the proximity of this area to the lake and Holocene erosion, but we note that we have yet to survey beyond Area 104 and similar deposits may well be discovered elsewhere around Koobi Fora.

4.2. Synthesis of GaJj17 evidence with previous findings

As our work highlights, the behavioral and ecological association of finds needs to be demonstrated rather than assumed. Instances of surface artifacts considered to share affinity with dated Late Pleistocene artifacts [e.g., bifacial hierarchical cores and associated triangular flakes (Shea, 2020)] are common in Turkana (Kelly, 1996a; Shea and Hildebrand, 2010). Despite their common occurrence, very little research has been

conducted to determine their stratigraphic provenience and the depositional history therein.

Kelly and Harris (1992) described multiple sites in the Ileret sub-region (FxJj 1, 2 and 3) and in the Karari region (FxJj 62 and 66). In Alia Bay, Kelly's field notes and our own observations from walking survey indicate the presence of MSA stone artifacts, but no evidence for *in situ* evidence currently exists. On the western margin of Lake Turkana, Shea and Hildebrand (2010) reported multiple occurrences of MSA sites, including Nakechikchok and Kadokorinyang (Fig. 1). Expansive exposures considered Late Pleistocene in age occur in this region and chronological refinement is ongoing (Wright personal communication, Shea personal communication).

Facies analysis, structural measurements, and elevation data obtained from dGPS have enabled our investigation of the broad stratigraphic and depositional history of landscape evolution at Koobi Fora with a focus on Middle and Late Pleistocene deposits within the Koobi Fora Formation and its interaction with underlying geology. Preliminary results from these investigations, in conjunction with our excavation results, point to the presence of a laterally continuous Late Pleistocene paleosurface in the eastern Turkana Basin. While current results record its presence only at Koobi Fora, it is likely that these deposits formed across the ancient Turkana Basin landscape. Additional sedimentological and stratigraphic work is ongoing to confirm this, particularly near Karari, and at Post-Chari Member near-shore localities such as those at Ileret.

Poor surface preservation of the bones, high fragmentation, small sample size, and lack of comparability with published datasets hinders a more complete understanding of the GaJj17 fish assemblage. Archaeological assemblages differ in species representation from both modern naturally occurring sites as well as modern human-accumulated assemblages (Stewart, 1991) due to processes related to site formation (e.g., attrition). At human-accumulated sites a smaller diversity of fish dominates due to preferential selection by humans (Gifford-Gonzalez et al., 1999). Modern non-human accumulated fish assemblages also differ from the taxonomic diversity of the modern lake today, as Stewart (1991) shows, with several species of ray-finned fish overrepresented and others underrepresented in comparison to the relative abundance of species in the lake; this differential relative abundances of fish species, Stewart (1991) suggests, may be explained by an overrepresentation of littoral taxa at the sites she excavated, as well as the fragility of the bones of some taxa and a size bias. While our analyses were not conclusive regarding the accumulating agent of aquatic faunal remains at GaJj17, our results contribute to the limited literature on fish remains from archaeological sites in the Pleistocene. We hope our study will be useful for future research interpreting early fishing practices and the role of aquatic resources in the evolution of *Homo sapiens*. Furthermore, as Joordens et al. argued, "the default assumption (…) should be that omnivorous hominids who lived in (…) habitats with catchable aquatic fauna could have consumed aquatic resources" (2009:667). Hominins have been opportunistic feeders through most of their evolution (Archer and Braun, 2013; Archer et al., 2014; Braun et al., 2010; Erlandson, 2001; Joordens et al., 2009; Steele, 2010), and it seems unlikely that Late Pleistocene humans living by Lake Turkana would have ignored the availability of such resources.

5. Site formation and later Pleistocene archaeology in the Omo-Turkana Basin

The scale of our behavioral questions is conditioned on the scale of environmental and temporal variation represented in the sediments available for study. The lack of radiocarbon dating options at GaJj17, for example, reflects the nature of working in arid regions with poor collagen preservation and the importance of continued sedimentological work integrating OSL, tephrochronology, and other geochronological methods. The unconsolidated nature of the sands, which overlie disconformable surfaces and are overall patchy in nature, can be studied by expanding laterally and sampling patches at different places in the basin. By describing the depositional and archaeological formation processes at GaJj17 we contribute here toward reconstruction of later Pleistocene site formation, preservation, and visibility in Turkana; these data are crucial for future site prospecting and paleolake modeling research in Turkana, both of which are necessary for understanding more broadly how humans utilized, and adapted to, dynamic ecologies in the Rift Valley.

It remains unclear whether the archaeological evidence at GaJj17 is the result of a short pulse of human habitation or was part of a longer more extensive occupation history obscured by a lack of a high-resolution stratigraphy. While GaJj17 alone cannot answer this question, it does emphasize the significance of this region and period for understanding the evolutionary history of human adaptations to lacustrine environments. Multiple lines of evidence indicate that Lake Turkana underwent extensive and sometimes extreme lake fluctuations throughout the Holocene. The Late Pleistocene record is less clear and may have been characterized by similar lake-level fluctuations. A landscape-scale sedimentological understanding of Middle and Late Pleistocene archaeological sites, building on the work of Vondra et al. (1971), Bowen and Vondra (1973), and Brown and Feibel (1986, 1991) will enable better contextualization of the occurrence of these Late Pleistocene sites across space and their stratigraphic relationships.

Author contributions

All authors made substantial contributions to this submission. Ranhorn led the research idea, planning, integration of analyses, and writing. Mavuso led sedimentology research in collaboration with Warren, Colarossi led luminescence dating, Dogandžić helped facilitate excavations in 2016 and site formation analysis along with Ssebuyungo and Ranhorn, O'Brien led terrestrial faunal analysis while Ribordy led aquatic faunal study. Braun is a co-PI of the Koobi Fora Research and Training Program (KFRPT) and leads US-based research and education programs, along with co-author E. Ndiema, co-PI of the KFRPT and expert in later quaternary archaeology of Turkana. Harris led initial work in this area and provided vital guidance throughout. All authors approved the final version of the manuscript.

Declaration of competing interest

The authors declare that they have no known competing financial interests or personal relationships that could have appeared to influence the work reported in this paper.

Data availability

Data will be made available on request.

Acknowledgements

We are deeply indebted to Alison Kelly whose meticulous documentation enabled this work to be conducted and we dedicate this paper to her memory. Peter Onyango, David Kipkebut, and Ben Sila were instrumental in the re-excavation of GaJj17. We thank the Koobi Fora Research and Training Program (KFRTP) and the National Museums of Kenya for providing the logistical support needed to make this field research possible. Bridget Murray, Chloe Daniel, Logan Van Hagen, Courtney Jirsa, Ella Beaudoin, and Michael Ziegler all assisted in the excavation of GaJj17. Jonathan Reeves provided valuable assistance with aerial imagery. The OSL samples were prepared by Katharina Schilling. Research was conducted with NACOSTI research clearance and was funded by NSF International Research Experience (OISE 1358178 and 1358200) and NSF Archaeology (BCS 1624398). TD and DC thank Max Planck Gesellschaft and Jean-Jacques Hublin for supporting their research. KR is grateful to Christian Tryon for support

during the initial write up of this work. We also thank the Palaeontological Scientific Trust (PAST), DSI-NRF Centre of Excellence in Palaeosciences (GENUS), Harvard University Department of Anthropology, the Turkana Basin Institute, the Leakey Foundation and the Wenner-Gren Foundation for generous funding of this research.

Appendix A. Supplementary data

Supplementary data to this article can be found online at https://doi.org/10.1016/j.quascirev.2023.108257.

References

Adams, A.E., Mackenzie, W.S., Guilford, C., 1984. Atlas of Sedimentary Rocks under the Microscope. Longman, Harlow.
Ambrose, S.H., 2002. Small things remembered: origins of early microlithic industries in sub-Saharan Africa. In: Elston, R.G., Kuhn, S.L. (Eds.), Thinking Small: Global Perspectives on Microlithization. Archaeological Papers of the American Anthropological Association No. 12, pp. 9–29.
Archer, W., Braun, D.R., 2013. Investigating the signature of aquatic resource use within Pleistocene hominin dietary adaptations. PLoS One 8, e69899.
Archer, W., Braun, D.R., Harris, J.W., McCoy, J.T., Richmond, B.G., 2014. Early Pleistocene aquatic resource use in the Turkana Basin. J. Hum. Evol. 77, 74–87.
Auclair, M., Lamothe, M., Huot, S., 2003. Measurement of anomalous fading for feldspar IRSL using SAR. Radiat. Meas. 37, 487–492.
Behrensmeyer, A.K., 1978. Taphonomic and ecologic information from bone weathering. Paleobiology 4, 150–162.
Beverly, E.J., White, J.D., Peppe, D.J., Faith, J.T., Blegen, N., Tryon, C.A., 2020. Rapid Pleistocene desiccation and the future of africa's Lake Victoria. Earth Planet Sci. Lett. 530, 115883.
Beyin, A., Prendergast, M.E., Grillo, K.M., Wang, H., 2017. New radiocarbon dates for terminal Pleistocene and early Holocene settlements in West Turkana, northern Kenya. Quat. Sci. Rev. 168, 208–215.
Blegen, N., Tryon, C.A., Faith, J.T., Peppe, D.J., Beverly, E.J., Li, B., Jacobs, Z., 2015. Distal tephras of the eastern Lake Victoria basin, Equatorial East Africa: correlations, chronology, and a context for early modern humans. Quat. Sci. Rev. 122, 89–111.
Bloszies, C., Forman, S., Wright, D., 2015. Water level history for Lake Turkana, Kenya in the past 15,000 years and a variable transition from the african humid period to Holocene aridity. Global Planet. Change 132, 64–76.
Bobe, R., Behrensmeyer, A.K., 2004. The expansion of grassland ecosystems in Africa in relation to mammalian evolution and the origin of the genus *Homo*. Palaeogeogr. Palaeoclimatol. Palaeoecol. 207, 399–420.
Boëda, É., 1995. Levallois: A Volumetric Concept, Methods, A Technique. In: Dibble, H. L., Bar-Yosef, O. (Eds.), The Definition and Interpretation of Levallois Technology. Prehistory Press, Madison, WI, pp. 41–68.
Bøtter-Jensen, L., Andersen, C.E., Duller, G.A.T., Murray, A.S., 2003. Developments in radiation, stimulation and observation facilities in luminescence measurements. Radiat. Meas. 37.
Bowen, B.E., Vondra, C.F., 1973. Stratigraphical relationships of the plio-pleistocene deposits, East rudolf, Kenya. Nature 242, 391.
Brauer, G., Leakey, R., Mbua, E., 1992. A first report on the KNM-ER 3884 cranial remains from Ileret/East Turkana, Kenya. Continuity or Replacement. In: Controversies in Homo sapiens Evolution, 111119.
Braun, D.R., Harris, J.W., Levin, N.E., McCoy, J.T., Herries, A.I., Bamford, M.K., Bishop, L.C., Richmond, B.G., Kibunjia, M., 2010. Early hominin diet included diverse terrestrial and aquatic animals 1.95 Ma in East Turkana, Kenya. In: Proceedings of the National Academy of Sciences, 201002181.
Braun, D.R., Levin, N.E., Stynder, D., Herries, A.I.R., Archer, W., Forrest, F., Roberts, D. L., Bishop, L.C., Matthews, T., Lehmann, S.B., Pickering, R., Fitzsimmons, K.E., 2013. Mid-pleistocene hominin occupation at elandsfontein, western Cape, South Africa. Quat. Sci. Rev. 82, 145–166.
Brown, F.H., Feibel, C.S., 1986. Revision of lithostratigraphic nomenclature in the Koobi Fora region, Kenya. J. Geol. Soc. 143, 297–310. London.
Brown, F.H., Feibel, C.S., 1991. Stratigraphy, depositional environments and paleogeography of the Koobi Fora Formation. In: Harris, J.M. (Ed.), Koobi Fora Research Project, Volume 3. Stratigraphy, Artiodactyls and Paleoenvironments. Clarendon Press, Oxford, pp. 1–30.
Bullock, P., Fedoroff, N., Jongerius, A., Stoops, G., Tursina, T., 1985. Handbook for Soil Thin Section Description. Waine Research.
Burrough, S.L., Thomas, D.S., Shaw, P.A., Bailey, R.M., 2007. Multiphase quaternary highstands at lake Ngami, Kalahari, northern Botswana. Palaeogeogr. Palaeoclimatol. Palaeoecol. 253, 280–299.
Bushozi, P.M., Skinner, A., de Luque, L., 2020. The middle stone age (MSA) technological patterns, innovations, and behavioral changes at bed VIA of Mumba rockshelter, northern Tanzania. Afr. Archaeol. Rev. 1–18.
Cahen, D., Moeyersons, J., 1977. Subsurface movements of stone artefacts and their implications for the prehistory of Central Africa. Nature 266, 812–815.
Carr, A.S., Armitage, S.J., Berrío, J.-C., Bilbao, B.A., Boom, A., 2016. An optical luminescence chronology for late Pleistocene aeolian activity in the Colombian and Venezuelan Llanos. Quat. Res. 85, 299–312.
Carr, A.S., Hay, A.S., Powell, D.M., Livingstone, I., 2019. Testing post-IR IRSL luminescence dating methods in the southwest Mojave Desert, California, USA. Quat. Geochronol. 49, 85–91.
Cerasoni, J.N., 2021. Vectorial application for the illustration of archaeological lithic artefacts using the "stone tools illustrations with vector art"(STIVA) method. PLoS One 16, e0251466.
Cerling, T.E., Wynn, J.G., Andanje, S.A., Bird, M.I., Korir, D.K., Levin, N.E., Mace, W., Macharia, A.N., Quade, J., Remien, C.H., 2011. Woody cover and hominin environments in the past 6 million years. Nature 476, 51–56.
Cohen, K.M., Finney, S.C., Gibbard, P.L., Fan, J.-X., 2013. The ICS international chronostratigraphic chart. Episodes 36, 199–204.
Colarossi, D., Duller, G., Roberts, H., 2018. Exploring the behaviour of luminescence signals from feldspars: implications for the single aliquot regenerative dose protocol. Radiat. Meas. 109, 35–44.
d'Errico, F., Martí, A.P., Shipton, C., Le Vraux, E., Ndiema, E., Goldstein, S., Petraglia, M. D., Boivin, N., 2020. Trajectories of cultural innovation from the middle to later stone age in eastern Africa: personal ornaments, bone artifacts, and ocher from Panga ya Saidi, Kenya. J. Hum. Evol. 141, 102737.
Davis, C.A., 2019. Foraging along Blue Highways: Seasonality and Subsistence Strategies in the Middle Stone Age of Ethiopia. The University of Texas at Austin.
Day, M., Leakey, R., 1974. New evidence of the genus Homo from East rudolf, Kenya (III). Am. J. Phys. Anthropol. 41, 367–380.
Deer, W.A., Howie, R.A., Zussman, J., 1992. An Introduction to the Rock-Forming Minerals, second ed. Longman Scientific & Technical, London.
Dibble, H.L., McPherron, S.P., 1996. A Multimedia Companion to the Middle Paleolithic Site of Combe-Capelle Bas (France). CD-ROM. University of Pennsylvania.
Duller, G., 2015. The Analyst software package for luminescence data: overview and recent improvements. Ancient TL 33, 35–42.
Durcan, J.A., King, G.E., Duller, G.A.T., 2015. DRAC: dose rate and age calculator for trapped charge dating. Quat. Geochronol. 28, 54–61.
Erlandson, J.M., 2001. The archaeology of aquatic adaptations: paradigms for a new millennium. J. Archaeol. Res. 9, 287–350.
Feibel, C.S., 2011. A geological history of the Turkana Basin. Evol. Anthropol. Issues News Rev. 20, 206–216.
Feibel, C.S., 2013. Facies Analysis and Plio-Pleistocene Paleoecology, Early Hominin Paleoecology. University Press of Colorado, pp. 35–58.
Finney, B., Scholz, C., Johnson, T., Trumbore, S., 2019. Late Quaternary Lake-Level Changes of Lake Malawi, the Limnology, Climatology and Paleoclimatology of the East African Lakes. Routledge, pp. 495–508.
Forman, S.L., Wright, D.K., Bloszies, C., 2014. Variations in water level for Lake Turkana in the past 8500 years near Mt. Porr, Kenya and the transition from the african humid period to Holocene aridity. Quat. Sci. Rev. 97, 84–101.
Galbraith, R.F., 1990. The radial plot: graphical assessment of spread in ages. Int. J. Radiat. Appl. Instrum. Nucl. Tracks Radiat. Meas. 17, 207–214.
Garcea, E.A., 2022. The Stone Age of the Middle Nile Valley. Oxford Research Encyclopedia of Anthropology.
Garcin, Y., Melnick, D., Strecker, M.R., Olago, D., Tiercelin, J.-J., 2012. East African mid-Holocene wet–dry transition recorded in palaeo-shorelines of Lake Turkana, northern Kenya Rift. Earth Planet Sci. Lett. 331, 322–334.
Gathogo, P.N., Brown, F.H., 2006. Stratigraphy of the Koobi Fora Formation in the Ileret region of northern Kenya. J. Afr. Earth Sci. 45.
Gifford-Gonzalez, D., Stewart, K.M., Rybczynski, 1999. Human activities and site formation at modern lake margin foraging camps in Kenya. J. Anthropol. Archaeol. 18, 397–440.
Goldberg, P., 1979. Micromorphology of pech-de-l'Aze II sediments. J. Archaeol. Sci. 6, 17–47.
Guérin, G., Christophe, C., Philippe, A., Murray, A., Thomsen, K., Tribolo, C., Urbanova, P., Jain, M., Guibert, P., Mercier, N., Kreutzer, S., Lahaye, C., 2017. Absorbed dose, equivalent dose, measured dose rates, and implications for OSL age estimates: introducing the Average Dose Model. Quat. Geochronol. 41, 163–173.
Guérin, G., Mercier, N., Adamiec, G., 2011. Dose-rate conversion factors: update. Ancient TL 29, 5–8.
Harris, J.W.K., 1972. In: Kenya, N.M.o. (Ed.), Field Notes on the 1972 Season at Koobi Fora. Nairobi, Kenya.
Hogg, A.G., Heaton, T.J., Hua, Q., Palmer, J.G., Turney, C.S., Southon, J., Bayliss, A., Blackwell, P.G., Boswijk, G., Ramsey, C.B., 2020. SHCal20 Southern Hemisphere calibration, 0–55,000 years cal BP. Radiocarbon 62, 759–778.
Hublin, J.-J., Ben-Ncer, A., Bailey, S.E., Freidline, S.E., Neubauer, S., Skinner, M.M., Bergmann, I., Le Cabec, A., Benazzi, S., Harvati, K., 2017. New fossils from Jebel Irhoud, Morocco and the pan-African origin of Homo sapiens. Nature 546, 289.
Huntley, D.J., Baril, M., 1997. The K content of the K-feldspars being measured in optical dating or in thermoluminescence dating. Ancient TL 15, 11–13.
Huntley, D.J., Lamothe, M., 2001. Ubiquity of anomalous fading in K-feldspars and the measurement and correction for it in optical dating. Can. J. Earth Sci. 38, 1093–1106.
Inwood, J., 2022. East Africa Hit by Drought, yet Kenya's Lake Turkana Is Flooding. BBC.
Isaac, G.L., Leakey, R.E.F., Behrensmeyer, A.K., 1971. Archeological traces of early hominid activities, East of Lake Rudolf, Kenya. Science 173, 1129–1134.
Jongerius, A., Rutherford, G.K., 1979. Glossary of Soil Micromorphology. Centre for Agricultural Publishing and Documentation, Wageningen.
Joordens, J.C., Wesselingh, F.P., de Vos, J., Vonhof, H.B., Kroon, D., 2009. Relevance of aquatic environments for hominins: a case study from Trinil (Java, Indonesia). J. Hum. Evol. 57, 656–671.
Karkanas, P., Goldberg, P., 2013. Micromorphology of cave sediments. In: Shroder, J.F., Frumkin, S. (Eds.), Treatise on Geomorphology. Academic Press, San Diego, pp. 286–297.

Kelly, A.J., 1996a. Intra-regional and Inter-regional Variability in the East Turkana (Kenya) and Kenyan Middle Stone Age, Anthropology. Rutgers, New Brunswick, New Jersey, p. 515.
Kelly, A.J., 1996b. Recently recovered middle stone age assemblages from East Turkana, northern Kenya: their implications for understanding technological adaptations during the late Pleistocene. Kaupia 6, 47–55.
Kelly, A.J., Harris, J.W.K., 1992. Recent findings of middle stone age material from East Turkana. Nyame Akuma 38.
Leakey, M.D., 1970. Early artefacts from the Koobi Fora area. Nature 226, 228–230.
Leakey, R.E., Leakey, M.G., Behrensmeyer, A.K., 1978. The hominid catalogue. In: Leakey, M.G., Leakey, R.E. (Eds.), Koobi Fora Research Project 1: the Fossil Hominids and an Introduction to Their Context, 1968-1974. Oxford University Press, Oxford, pp. 86–182.
Leplongeon, A., 2016. Middle Stone Age and Early Late Stone Age Lithic Assemblages at Enkapune Ya Muto (Kenya).
Lomax, J., Hilgers, A., Radtke, U., 2011. Palaeoenvironmental change recorded in the palaeodunefields of the western Murray Basin, South Australia–new data from single grain OSL-dating. Quat. Sci. Rev. 30, 723–736.
Lomax, J., Hilgers, A., Twidale, C., Bourne, J., Radtke, U., 2007. Treatment of broad palaeodose distributions in OSL dating of dune sands from the western Murray Basin, South Australia. Quat. Geochronol. 2, 51–56.
Marean, C.W., 1992. Hunter to herder: large mammal remains from the hunter-gatherer occupation at Enkapune ya Muto rock-shelter, Central Rift, Kenya. Afr. Archaeol. Rev. 10, 65–127.
Marean, C.W., Mudida, N., Reed, K.E., 1994. Holocene paleoenvironmental change in the Kenyan central rift as indicated by micromammals from Enkapune Ya Muto rockshelter. Quat. Res. 41, 376–389.
Mayya, Y., Morthekai, P., Murari, M.K., Singhvi, A., 2006. Towards quantifying beta microdosimetric effects in single-grain quartz dose distribution. Radiat. Meas. 41, 1032–1039.
McBrearty, S., Brooks, A.S., 2000. The revolution that wasn't: a new interpretation of the origin of modern human behavior. J. Hum. Evol. 39, 453–563.
McBrearty, S., Tryon, C., 2006. From Acheulean to Middle Stone Age in the Kapthurin Formation, Kenya. In: Hovers, E., Kuhn, S.L. (Eds.), Transitions Before the Transition. Interdisciplinary Contributions To Archaeology. Springer, Boston, MA. https://doi.org/10.1007/0-387-24661-4_14.
McDougall, I., 1985. K-Ar and $^{40}Ar/^{39}Ar$ dating of the hominid-bearing pliocene-pleistocene sequence at Koobi Fora, Lake Turkana, northern Kenya. Geol. Soc. Am. Bull. 96, 159–175.
McDougall, I., Brown, F., 2006. Precise $^{40}Ar/^{39}Ar$ geochronology for the upper Koobi Fora Formation, Turkana Basin, northern Kenya. J. Geol. Soc. 163, 57–70. London.
McDougall, I., Brown, F.H., Fleagle, J.G., 2005. Stratigraphic placement and age of modern humans from Kibish, Ethiopia. Nature 433, 733–736.
McLaren, S., 2011. Aeolianite. In: Nash, D.J., McLaren, S. (Eds.), Geochemical Sediments and Landscapes. John Wiley and Sons.
McPherron, S.P., 2018. Additional statistical and graphical methods for analyzing site formation processes using artifact orientations. PLoS One 13, e0190195.
Mehlman, M.J., 1977. Excavations at Nasera rock, Tanzania. Azania 12, 111–118.
Mehlman, M.J., 1979. Mumba-Höhle revisited: the relevance of a forgotten excavation to some current issues in East African prehistory. World Archaeol. 11, 80–94.
Mejdahl, V., 1987. Internal radioactivity in quartz and feldspar grains. Ancient TL 5, 10–17.
Miall, A., 1996. The Geology of Fluvial Deposits. Springer, Berlin.
Miall, A.D., 2014. Fluvial Depositional Systems. Springer.
Nicholson, Sharon E., 2018. The ITCZ and the seasonal cycle over equatorial Africa. Bull. Am. Meteorol. Soc. 99 (2), 337–348.
Obiero, K., Wakjira, M., Gownaris, N., Malala, J., Keyombe, J.L., Ajode, M.Z., Smith, S., Lawrence, T., Ogello, E., Getahun, A., 2022. (In Press). Lake Turkana: status, challenges, and opportunities for collaborative research. J. Great Lake. Res. https://doi.org/10.1016/j.jglr.2022.10.007.
Pargeter, J., Brooks, A., Douze, K., Eren, M., Groucutt, H.S, McNeil, J., Mackay, A., Ranhorn, K., Scerri, E., Shaw, M., Tryon, C., Will, M., Leplongeon, A., 2023. Replicability in Lithic Analysis. Amer Antiq.
Patania, I., Porter, S.T., Keegan, W.F., Dihogo, R., Frank, S., Lewis, J., Mashaka, H., Ogutu, J., Skosey-Lalonde, E., Tryon, C.A., Niespolo, E.M., Colarossi, D., Ranhorn, K. L., 2022. Geoarchaeology and heritage management: identifying and quantifying multi-scalar erosional processes at Kisese II Rockshelter, Tanzania. Front. Earth Sci. 9.
Peet, R.K., 1974. The measurement of species diversity. Annu. Rev. Ecol. Systemat. 285–307.
Prendergast, M.E., Beyin, A., 2018. Fishing in a fluctuating landscape: terminal Pleistocene and early Holocene subsistence strategies in the Lake Turkana Basin, Kenya. Quat. Int. 471, 203–218.
Prendergast, M.E., Luque, L., Domínguez-Rodrigo, M., Diez-Martín, F., Mabulla, A.Z.P., Barba, R., 2007. New excavations at Mumba rockshelter, Tanzania. J. Afr. Archaeol. 5, 217–243.
Prendergast, M.E., Miller, J., Mwebi, O., Ndiema, E., Shipton, C., Boivin, N., Petraglia, M., 2023. Small game forgotten: late Pleistocene foraging strategies in eastern Africa, and remote capture at Panga ya Saidi, Kenya. Quat. Sci. Rev. 305, 108032.
Prescott, J.R., Hutton, J.T., 1994. Cosmic ray contributions to dose rates for luminescence and ESR dating: large depths and long-term time variations. Radiat. Meas. 23, 497–500.
Pye, K., Tsoar, H., 2008. Aeolian Sand and Sand Dunes. Springer Science & Business Media.
Ranhorn, K.L., Colarossi, D., Molel, S., Laird, M.F., Lewis, J.E., Mashaka, H., Niespolo, E., Porter, S.T., Sawchuk, E., Sharp, W.D., Tryon, C.A., Patania, I., 2023. Kisese II Rockshelter, Tanzania. In: Beyin, A., Wright, D.K., Wilkins, J., Olszewski, D.I. (Eds.), Handbook of Pleistocene Archaeology of Africa : Hominin behavior, geography, and chronology. Springer International Publishing, Cham, pp. 1069–1081.
Ranhorn, K.L., Tryon, C.A., 2018. New Pleistocene radiocarbon dates from Nasera rockshelter, Tanzania. J. Afr. Archaeol. 16, 211–222.
Reimann, T., Thomsen, K.J., Jain, M., Murray, A.S., Frechen, M., 2012. Single-grain dating of young sediments using the pIRIR signal from feldspar. Quat. Geochronol. 11, 28–41.
Reimer, P.J., Austin, W.E., Bard, E., Bayliss, A., Blackwell, P.G., Ramsey, C.B., Butzin, M., Cheng, H., Edwards, R.L., Friedrich, M., 2020. The IntCal20 Northern Hemisphere radiocarbon age calibration curve (0–55 cal kBP). Radiocarbon 62, 725–757.
Schick, K., 1986. Stone Age Sites in the Making: Experiments in the Formation and Transformation of Archaeological Occurrences, vol. 314. BAR International Series No., Oxford.
Scholz, C.A., Rosendahl, B., 1988. Low lake stands in Lakes Malawi and Tanganyika, East Africa, delineated with multifold seismic data. Science 240, 1645–1648.
Shea, J.J., 2008. The middle stone age archaeology of the lower Omo valley Kibish Formation: excavations, lithic assemblages, and inferred patterns of early Homo sapiens behavior. J. Hum. Evol. 55, 448–485.
Shea, J.J., 2020. Prehistoric Stone Tools of Eastern Africa: A Guide. Cambridge University Press.
Shea, J.J., Hildebrand, E.A., 2010. The Middle Stone Age of west Turkana, Kenya. J. Field Archaeol. 35, 355–364.
Shipton, C., Roberts, P., Archer, W., Armitage, S.J., Bita, C., Blinkhorn, J., Courtney-Mustaphi, C., Crowther, A., Curtis, R., Errico, F., Douka, K., Faulkner, P., Groucutt, H.S., Helm, R., Herries, A.I.R., Jembe, S., Kourampas, N., Lee-Thorp, J., Marchant, R., Mercader, J., Marti, A.P., Prendergast, M.E., Rowson, B., Tengeza, A., Tibesasa, R., White, T.S., Petraglia, M.D., Boivin, N., 2018. 78,000-year-old record of Middle and Later Stone Age innovation in an East African tropical forest. Nat. Commun. 9, 1832.
Singarayer, J., Bailey, R., 2003. Further investigations of the quartz optically stimulated luminescence components using linear modulation. Radiat. Meas. 37, 451–458.
Smedley, R., Duller, G., Rufer, D., Utley, J., 2020. Empirical assessment of beta dose heterogeneity in sediments: implications for luminescence dating. Quat. Geochronol. 56, 101052.
Smedley, R.K., Duller, G.A., Pearce, N., Roberts, H.M., 2012. Determining the K-content of single-grains of feldspar for luminescence dating. Radiat. Meas. 47, 790–796.
Smith, J.J., Hasiotis, S.T., Kraus, M.J., Woody, D.T., 2008. Relationship of floodplain ichnocoenoses to paleopedology, paleohydrology, and paleoclimate in the Willwood Formation, Wyoming, during the Paleocene-Eocene Thermal Maximum. Palaios 23 (10), 683–699.
Solano-Megías, I., Maíllo-Fernández, J.-M., Marín, J., Martín-Perea, D.M., Mabulla, A.Z., 2021. Lithic technology in the earliest later stone age at Nasera rockshelter (Tanzania). Lithic Technol. 46, 60–79.
Steele, J., 2010. Radiocarbon dates as data: quantitative strategies for estimating colonization front speeds adn event densities. J. Archaeol. Sci. 37, 2017–2030.
Stewart, K.M., 1991. Modern fishbone assemblages at Lake Turkana, Kenya: a methodology to aid in recognition of hominid fish utilization. J. Archaeol. Sci. 18, 579–603.
Stewart, K.M., Gifford-Gonzalez, D., 1994. An ethnoarchaeological contribution to identifying hominid fish processing sites. J. Archaeol. Sci. 21 (2), 237–248.
Stoops, G., 2003. Guidelines for Analysis and Description of Soil and Regolith Thin Sections. Soil Science Society of America Inc.
Stuiver, M., Reimer, P.J., 1993. Extended 14C data base and revised CALIB 3.0 14C age calibration program. Radiocarbon 35, 215–230.
Thiel, C., Buylaert, J.-P., Murray, A., Terhorst, B., Hofer, I., Tsukamoto, S., Frechen, M., 2011. Luminescence dating of the Stratzing loess profile (Austria) - testing the potential of an elevated temperature post-IR IRSL protocol. Quat. Int. 234, 23–31.
Thomas, D.S., Shaw, P.A., 2002. Late Quaternary environmental change in central southern Africa: new data, synthesis, issues and prospects. Quat. Sci. Rev. 21, 783–797.
Thomsen, K.J., Jain, M., Murray, A., Denby, P.M., Roy, N., Bøtter-Jensen, L., 2008. Minimizing feldspar OSL contamination in quartz UV-OSL using pulsed blue stimulation. Radiat. Meas. 43, 752–757.
Trinkaus, E., 1993. A note on the KNM-ER 999 hominid femur. J. Hum. Evol. 24, 493–504.
Tryon, C.A., 2010. How the geological record affects our reconstructions of Middle Stone Age settlement patterns: the case of alluvial fans in Baringo, Kenya. In: Conard, N., Delagnes, A. (Eds.), Settlement Dynamics of the Middle Paleolithic & Middle Stone Age, Volume III. Kerns Verlag, Tübingen, pp. 39–66.
Tryon, C.A., Faith, J.T., 2016. A demographic perspective on the Middle to Later Stone Age transition from Nasera rockshelter, Tanzania. Phil. Trans. Biol. Sci. B 371, 1–11.
Tryon, C.A., Faith, J.T., Peppe, D.J., Keegan, W.F., Keegan, K.N., Jenkins, K.H., Nightingale, S., Patterson, D., Van Plantinga, A., Driese, S., Johnson, C.R., Beverly, E. J., 2014. Sites on the landscape: paleoenvironmental context of Late Pleistocene archaeological sites from the Lake Victoria basin, equatorial East Africa. Quat. Int. 331, 20–30.
Tryon, C.A., Lewis, J.E., Ranhorn, K.L., Kwekason, A., Alex, B., Laird, M.F., Marean, C. W., Niespolo, E., Nivens, J., Mabulla, A.Z.P., 2018. Middle and Later Stone Age chronology of Kisese II Rockshelter (UNESCO World Heritage Kondoa rock-art sites), Tanzania. PLoS One 13, e0192029.
Tryon, C.A., McBrearty, S., 2002. Tephrostratigraphy and the Acheulian to Middle Stone Age transition in the Kapthurin Formation, Baringo, Kenya. J. Hum. Evol. 42, 211–235.

Tryon, C.A., McBrearty, S., Texier, P.-J., 2006. Levallois lithic technology from the Kapthurin Formation, Kenya: Acheulian origin and Middle Stone Age diversity. Afr. Archaeol. Rev. 22, 199–229.
Vermeersch, P.M., Van Neer, W., 2015. Nile behaviour and Late Palaeolithic humans in upper Egypt during the Late Pleistocene. Quat. Sci. Rev. 130, 155–167.
Vidal, C.M., Lane, C.S., Asrat, A., Barfod, D.N., Mark, D.F., Tomlinson, E.L., Tadesse, A.Z., Yirgu, G., Deino, A., Hutchison, W., 2022. Age of the oldest known Homo sapiens from eastern Africa. Nature 1–5.
Villa, P., Mahieu, E., 1991. Breakage patterns of human long bones. J. Hum. Evol. 21, 27–48.
Vondra, C.F., Johnson, G.D., Bowen, B.E., Behrensmeyer, A.K., 1971. Preliminary stratigraphical studies of the East Rudolf basin, Kenya. Nature 231, 245–248.
Wilkins, J., Brown, K.S., Oestmo, S., Pereira, T., Ranhorn, K.L., Schoville, B.J., Marean, C. W., 2017. Lithic technological responses to Late Pleistocene glacial cycling at Pinnacle Point Site 5-6, South Africa. PloS one 12, e0174051.
Will, M., Bader, G.D., Conard, N.J., 2014. Characterizing the Late Pleistocene MSA lithic technology of Sibudu, KwaZulu-Natal, South Africa. PLoS One 9, e98359.
Willis, L.M., Eren, M.I., Rick, T.C., 2008. Does butchering fish leave cut marks? J. Archaeol. Sci. 35, 1438–1444.
Wilson, A., Flint, S., Payenberg, T., Tohver, E., Lanci, L., 2014. Architectural styles and sedimentology of the fluvial lower beaufort group, Karoo Basin, South Africa. J. Sediment. Res. 84, 326–348.
Wood, B., Leakey, M., 2011. The Omo-Turkana Basin fossil hominins and their contribution to our understanding of human evolution in Africa. Evol. Anthropol. Issues News Rev. 20, 264–292.